Microgravity-Science and Technology (2018) 30:209–228
https://doi.org/10.1007/s12217-017-9591-4

ORIGINAL ARTICLE

Longwave Stability of Two Liquid Layers Coating Both Sides of a Thick Wall in the Absence of Gravity

L. A. Dávalos-Orozco[1]

Received: 2 March 2017 / Accepted: 22 December 2017 / Published online: 4 January 2018
© Springer Science+Business Media B.V., part of Springer Nature 2018

Abstract
A system of two coupled nonlinear equations was calculated to describe the thermocapillary evolution of the free surface deformations of two liquid layers coating both sides of a wall of finite thickness and thermal conductivity in the absence of gravity. The equations were obtained under the small wavenumber approximation. A temperature gradient appears perpendicular to the liquid-wall-liquid system due to the temperature difference between the atmospheres outside the free surfaces of both fluid layers. The linear growth rate of the system was investigated with respect to a variety of parameters. Under some conditions, two stationary modes and one oscillatory mode between them were found. The second stationary mode was concluded to be always stable. It was also found that under different conditions only stationary convection is possible. These results depended on the relative thickness of the two fluid films. It is of interest to know if the coupled free surface perturbations presented a nonlinear sinuous or varicose mode. Thus, a two-dimensional numerical analysis was performed to find out which conditions lead to the sinuous or to the varicose mode of instability.

Keywords Thin liquid film · Thermocapillarity · Marangoni convection · Solid interlayer · Small wavenumber approximation

Introduction

Liquid films are susceptible to thermocapillary instabilities due to temperature differences between the substrate and the atmosphere. It has been shown by Pearson (1958) that after a large enough temperature difference, represented by the Marangoni number Ma, the liquid layer destabilizes if it is heated from the wall. On the contrary, if it is cooled from the wall (negative Marangoni number) the layer is always stable. These results were obtained assuming that the free surface was flat. Free surface deformations were first introduced by Scriven and Sternling (1964). It was found that the critical temperature difference, or the critical Marangoni number Ma_C, needed for instability was smaller than that of the flat surface. It was also found that when cooling from the wall, $Ma < 0$, the layer is always stable. The effects of gravity, in the absence of natural convection, were first taken into account by Takashima (1981a, b) in the stationary and time dependent case, respectively. Gravity has a restoring effect on the free surface deformation. However, in the oscillatory case some perturbations may destabilize when $Ma < 0$ Takashima (1981b). For a flat free surface, the double diffusive problem was investigated by Mctaggart (1983) and the viscoelastic problem by Getachew and Rosenblat (1985). When the viscosity depends on temperature the stability changes as shown in Slavtchev and Ouzounov (1994), Kalitzova-Kurteva et al. (1996) and by Slavtchev et al. (1998) for stationary and oscillatory Marangoni convection with a deformable free surface. These phenomena have also been investigated by Dávalos-Orozco and You (2000) and by Moctezuma-Sánchez and Dávalos-Orozco (2015) but for a cylindrical geometry.

In experiments the substrate has finite thickness and thermal conductivity, characteristics not always taken into account. Therefore, research including those wall properties has been done by Takashima (1970), Yang (1992), Char and Chen (1999), Gangadharaiah (2013) and by Hernández Hernández and Dávalos-Orozco (2015) for a viscoelastic

✉ L. A. Dávalos-Orozco
ldavalos@unam.mx

[1] Instituto de Investigaciones en Materiales, Departamento de Polímeros, Universidad Nacional Autónoma de México, Ciudad Universitaria, Circuito Exterior S/N, Delegación Coyoacán, 04510 Ciudad de México, México

fluid. This subject has also been investigated by Dávalos-Orozco (2012, 2014, 2015, 2016) for liquid films flowing down walls.

Thermocapillarity was investigated in two stratified liquid layers in the presence of buoyancy by Simanovskii et al. (2015, 2016). In contrast, the problem of two fluid layers under buoyancy effects alone but separated by a solid interlayer was investigated by Catton and Lienhard (1984) and Lienhard and Catton (1986). These last two papers showed that the thermal interaction of the two fluid layers when heated from below. For some magnitudes of the parameters the two fluid layers present natural convection, for other values only one is unstable.

The investigation of the thermal interaction of two fluid layers coating both sides of a solid interlayer when subjected to thermocapillary convection is the purpose of the present paper. The motivation is a theoretical investigation of an outer space experiment in a manned artificial satellite. It is assumed that the two liquid films present surface deformation. Therefore, the thermal interaction of both deformations may result in the formation of a sinuous or a varicose mode of instability, as found in the problem of liquid sheets. In the varicose mode the perturbations are out of phase by 180 degrees. Publications related with this problem are those by Oron et al. (1995a, b), Dávalos-Orozco (1999), Fu et al. (2013) and Tong et al. (2014). Similar conditions occur when the liquid layer is coating a deformable membrane Dávalos-Orozco (2001). The relevance of one kind of the two instability modes is determined in the nonlinear solution and depends on the parameters of the system.

The next section contains the description of the problem and the equations of motion along with their boundary conditions. The numerical results for the linear case are shown in "Linear Stability". The nonlinear modes of instability are investigated in "Nonlinear Sinuous and Varicose Modes of Instability". The conclusions are given in "Conclusions".

Two Liquid Layers Coating Both Sides of a Solid Wall

The system under research consists of two liquid layers coating both sides of a solid wall with finite thickness and thermal conductivity. The free surfaces of the fluids are allowed to deform. In non-dimensional form the system is sketched in Fig. 1. Gravity is assumed to be zero.

The z-axis is perpendicular to the wall and the x-axis is located at the interface of fluid 2 and the wall. The y-axis is perpendicular to both of them in a right-handed frame of reference. The mean non-dimensional thickness of fluid 2 is one, the mean non-dimensional thickness of fluid 1 is d and the non dimensional thickness of the wall is d_W.

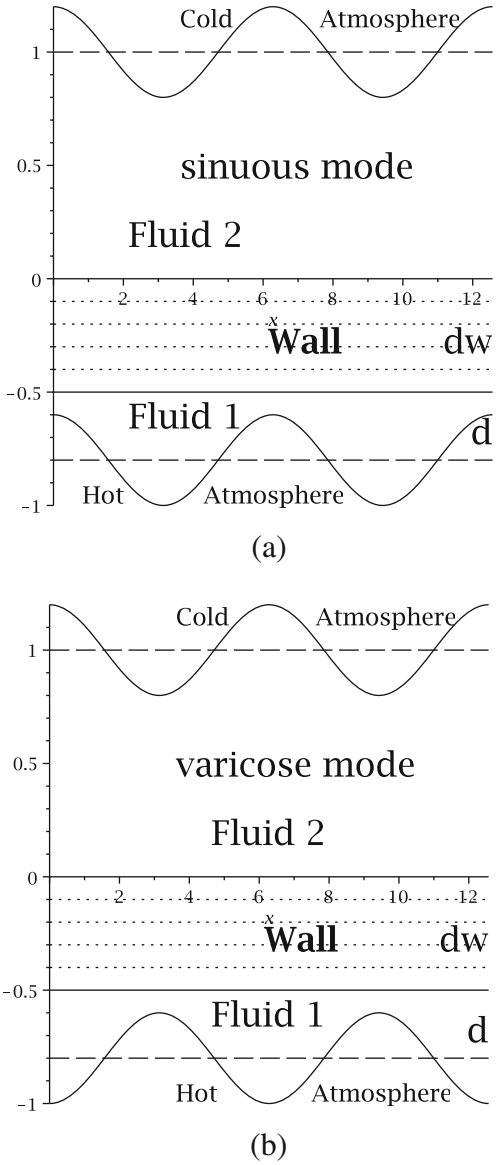

Fig. 1 Two sketches of the system. **a** sinuous mode. **b** varicose mode

In Fig. 1a and b it was assumed that the atmosphere below the free surface of fluid 1 was hotter than that above fluid 2. For a sufficiently large temperature difference one of the fluid layers (that of fluid 2) starts to move due to thermocapillary convection. However, the other one (which in other circumstances should be stable), feels the perturbations of the unstable layer through the solid interlayer and is also able to move. In other words, the stability of the two fluid layers depends on the coupling they have through the solid wall.

The equations of the two fluids and the wall and their corresponding boundary conditions were made non dimensional as follows. The distance in the z-direction was measured with d_2 the thickness of fluid 2, the distance in the x- and y-direction by $\lambda/2\pi = d_2/\varepsilon$, where λ was a

representative longitude of the free surface deformation. The time was scaled with $(\lambda/2\pi)^2/\alpha_2 = d_2^2/\varepsilon^2\alpha_2$ where α_2 is the thermal diffusivity of fluid 2, velocity with α_2/d_2 and pressure with $\rho_2\alpha_2\nu_2/d_2^3$ where ρ_2 and ν_2 are the density and the kinematic viscosity of fluid 2, respectively. The temperature was scaled with $\Delta\mathrm{T} = \mathrm{T}_L - \mathrm{T}_U$, where T_L is the temperature of the atmosphere below fluid 1 and T_U is the temperature of the atmosphere above fluid 2. The small parameter $\varepsilon = 2\pi\mathrm{d}_2/\lambda$ was used to scale the equations of motion and boundary conditions. It was assumed that in the small wavenumber approximation $\varepsilon < 1$.

According to the lubrication approximation (see Oron et al. 1997), the expansions of the non-dimensional dependent variables in terms of ε are

$$\begin{aligned} u &= \varepsilon(u_0 + \varepsilon u_1 + \cdots),\ v = \varepsilon(v_0 + \varepsilon v_1 + \cdots),\\ w &= \varepsilon^2(w_1 + \varepsilon w_2 + \cdots),\\ p &= p_0 + \varepsilon p_1 + \cdots,\ T = T_0 + \varepsilon T_1 + \cdots,\\ T_w &= T_{w0} + \varepsilon T_{w1} + \cdots. \end{aligned} \tag{1}$$

$$\begin{aligned} u_1 &= \varepsilon(u_{10} + \varepsilon u_{11} + \cdots),\ v_1 = \varepsilon(v_{10} + \varepsilon v_{11} + \cdots),\\ w_1 &= \varepsilon^2(w_{11} + \varepsilon w_{12} + \cdots),\\ p_1 &= p_{10} + \varepsilon p_{11} + \cdots,\ T_1 = T_{10} + \varepsilon T_{11} + \cdots. \end{aligned} \tag{2}$$

Under this lubrication approximation, the Marangoni and surface tension numbers defined below do not need an expansion in terms of ε. As will be seen presently, the reason is that the surface tension number appears in the pressure at the lowest order and no further approximation of the pressure is needed. The Marangoni number appears for the first time at the first order of the velocity boundary condition and the velocity does not need a further approximation (see Dávalos-Orozco 2012, 2014, 2015, 2016). The scaled non dimensional equations of motion, continuity and heat transfer of fluid 2 are:

$$\frac{1}{Pr}\left(\varepsilon^2 u_t + \varepsilon u u_x + \varepsilon v u_y + w u_z\right) = -\varepsilon p_x + \varepsilon^2 u_{xx} + \varepsilon^2 u_{yy} + u_{zz}. \tag{3}$$

$$\frac{1}{Pr}\left(\varepsilon^2 v_t + \varepsilon u v_x + \varepsilon v v_y + w v_z\right) = -\varepsilon p_y + \varepsilon^2 v_{xx} + \varepsilon^2 v_{yy} + v_{zz}. \tag{4}$$

$$\frac{1}{Pr}\left(\varepsilon^2 w_t + \varepsilon u w_x + \varepsilon v w_y + w w_z\right) = -p_z + \varepsilon^2 w_{xx} + \varepsilon^2 w_{yy} + w_{zz}. \tag{5}$$

$$w_z = -\varepsilon u_x - \varepsilon v_y. \tag{6}$$

$$\varepsilon^2 T_t + \varepsilon u T_x + \varepsilon v T_y + w T_z = \varepsilon^2 T_{xx} + \varepsilon^2 T_{yy} + T_{zz}. \tag{7}$$

The scaled non dimensional equations of motion, continuity and heat transfer of fluid 1 are:

$$\frac{1}{Pr}\left(\varepsilon^2 u_{1t} + \varepsilon u_1 u_{1x} + \varepsilon v_1 u_{1y} + w_1 u_{1z}\right) = -\frac{\varepsilon}{\rho} p_{1x} + \frac{\mu}{\rho}\left(\varepsilon^2 u_{1xx} + \varepsilon^2 u_{1yy} + u_{1zz}\right). \tag{8}$$

$$\frac{1}{Pr}\left(\varepsilon^2 v_{1t} + \varepsilon u_1 v_{1x} + \varepsilon v_1 v_{1y} + w_1 v_{1z}\right) = -\frac{\varepsilon}{\rho} p_{1y} + \frac{\mu}{\rho}\left(\varepsilon^2 v_{1xx} + \varepsilon^2 v_{1yy} + v_{1zz}\right). \tag{9}$$

$$\frac{1}{Pr}\left(\varepsilon^2 w_{1t} + \varepsilon u_1 w_{1x} + \varepsilon v_1 w_{1y} + w_1 w_{1z}\right) = -\frac{1}{\rho} p_{1z} + \frac{\mu}{\rho}\left(\varepsilon^2 w_{1xx} + \varepsilon^2 w_{1yy} + w_{1zz}\right). \tag{10}$$

$$w_{1z} = -\varepsilon u_{1x} - \varepsilon v_{1y}. \tag{11}$$

$$\varepsilon^2 T_{1t} + \varepsilon u_1 T_{1x} + \varepsilon v_1 T_{1y} + w_1 T_{1z} = \alpha\left(\varepsilon^2 T_{1xx} + \varepsilon^2 T_{1yy} + T_{1zz}\right). \tag{12}$$

and the equation of the temperature of the solid wall is:

$$\varepsilon^2 T_{wt} = \frac{\chi}{\frac{\rho_w}{\rho_2}\frac{c_{pw}}{c_{p2}}}\left(\varepsilon^2 T_{wxx} + \varepsilon^2 T_{wyy} + T_{wzz}\right). \tag{13}$$

where T, T_1 and T_w are the temperatures of fluid 2, fluid 1 and wall, respectively. Here, (u, v, w), (u_1, v_1, w_1) are the velocity vectors of fluid 2 and fluid 1. p and p_1 are the pressures of fluid 2 and fluid 1, respectively. $\mathrm{Pr} = \nu_2/\alpha_2$ is the Prandtl number, $\rho = \rho_1/\rho_2$, $\mu = \mu_1/\mu_2$ and $\alpha = \alpha_1/\alpha_2$, where ρ_1, μ_1 and α_1 are the density, dynamic viscosity and thermal diffusivity of fluid 1, respectively. In the equation of heat diffusion in the wall there are the following parameters: $\chi = \mathrm{K}_w/\mathrm{K}_2$ where K_w is the thermal conductivity of the wall, K_2 is the thermal conductivity of fluid 2, ρ_w is the density of the wall and c_{pw} is the heat capacity of the wall.

The boundary conditions for the velocity and temperature in fluid 2 were as follows. The fluid sticks to the wall. Then

$$u = v = w = 0. \qquad \text{at } z = 0 \tag{14}$$

The normal stress boundary condition at the free surface was

$$\begin{aligned} &-p + P_U - \frac{2}{N^2}[\varepsilon^3(u_x h_x^2 + v_y h_y^2) + \varepsilon^3(u_y + v_x)h_x h_y \\ &-\varepsilon(v_z + \varepsilon w_y)h_y - \varepsilon(u_z + \varepsilon w_x)h_x + w_z] \\ &= \frac{1}{N^3} S\left[(1 + \varepsilon^2 h_y^2)h_{xx} + (1 + \varepsilon^2 h_x^2)h_{yy} - 2\varepsilon^2 h_x h_y h_{xy}\right]. \\ &\text{at } z = h(x, y, t) \end{aligned} \tag{15}$$

where $N = \sqrt{1 + \varepsilon^2 h_x^2 + \varepsilon^2 h_y^2}$, $h(x, y, t) = 1 + H(x, y, t)$ and $H(x, y, t)$ is the free surface deformation of fluid 2.

Besides, P_U is the pressure of the atmosphere outside fluid 2 and $S = \varepsilon^2\gamma_2 d_2/\rho_2\nu_2\alpha_2$ is the scaled surface tension number and γ_2 is the surface tension of fluid 2. The balance of shear stresses and surface tension temperature gradients on the free surface was represented by the shear stress conditions in two directions. The first shear stress boundary condition was:

$$\frac{1}{N}\left[\varepsilon(w_z-\varepsilon u_x)h_x-\frac{1}{2}\varepsilon^2(u_y+v_x)h_y+\frac{1}{2}(u_z+\varepsilon w_x)(1-\varepsilon^2h_x^2)\right.$$
$$\left.-\frac{1}{2}\varepsilon^2(\varepsilon w_y+v_z)h_xh_y\right]=-Ma(\varepsilon T_x+\varepsilon h_xT_z). \qquad \text{at } z=h(x,y,t) \tag{16}$$

and the second shear stress boundary condition was:

$$\frac{1}{N}\left[\varepsilon h_y\left(\varepsilon^3u_xh_x^2-\varepsilon v_y\left(1+\varepsilon^2h_x^2\right)+w_z\right)\right.$$
$$+\frac{1}{2}\varepsilon^2\left(u_y+v_x\right)h_x\left(\varepsilon^2h_y^2-1-\varepsilon^2h_x^2\right)$$
$$-\varepsilon^2\left(\varepsilon w_x+u_z\right)h_xh_y+\frac{1}{2}\left(\varepsilon w_y+v_z\right)\left(1+\varepsilon^2h_x^2-\varepsilon^2h_y^2\right)\Big]$$
$$=-\frac{Ma}{N}\left[-\varepsilon^3T_xh_xh_y+\varepsilon T_y\left(1+\varepsilon^2h_x^2\right)+\varepsilon T_zh_y\right].$$
$$\text{at } z=h(x,y,t) \tag{17}$$

where $\mathrm{Ma} = -(d\gamma_2/dT)\Delta T d_2/2\rho_2\nu_2\alpha_2$ is the Marangoni number of fluid 2. The kinematic boundary condition of fluid 2 was

$$\varepsilon^2h_t+\varepsilon uh_x+\varepsilon vh_y-w=0. \qquad \text{at } z=h(x,y,t) \tag{18}$$

The boundary conditions of the temperature of fluid 2 and the wall are the following. At the free surface

$$\frac{1}{N}\left(\varepsilon h_xT_x+\varepsilon h_yT_y-T_z\right)=BiT. \qquad \text{at } z=h(x,y,t) \tag{19}$$

$$T=T_w \qquad \text{and } T_z=\chi T_{wz}. \qquad \text{at } z=0 \tag{20}$$

where $\mathrm{Bi} = Q_{h2}d_2/K_2$ is the Biot number and Q_{h2} is the heat transfer coefficient at the interface of fluid 2.

The boundary conditions for the velocity and temperature of fluid 1 were as follows. Again, the fluid sticks to the wall. Therefore

$$u_1=v_1=w_1=0. \qquad \text{at } z=-d_w \tag{21}$$

The normal stress boundary condition at the free surface was

$$-p_1+P_L-\frac{2\mu}{N_1^2}[\varepsilon^3(u_{1x}h_{1x}^2+v_{1y}h_{1y}^2)+\varepsilon^3(u_{1y}+v_{1x})h_{1x}h_{1y}$$
$$+\varepsilon(v_{1z}+\varepsilon w_{1y})h_{1y}+\varepsilon(u_{1z}+\varepsilon w_{1x})h_{1x}+w_{1z}]$$
$$=\frac{\gamma S}{N_1^3}[(1+\varepsilon^2h_{1y}^2)h_{1xx}+(1+\varepsilon^2h_{1x}^2)h_{1yy}-\varepsilon^2h_{1x}h_{1y}h_{1xy}].$$
$$\text{at } z=-d_w-h_1(x,y,t) \tag{22}$$

where $N_1 = \sqrt{1+\varepsilon^2h_{1x}^2+\varepsilon^2h_{1y}^2}$, $h_1(x,y,t) = \mathrm{d} + H_1(x,y,t)$ and $H_1(x,y,t)$ is the free surface deformation of fluid 1. Besides, P_L is the pressure of the atmosphere outside fluid 1 and $\gamma = \gamma_1/\gamma_2$ where γ_1 is surface tension of fluid 1. The balance of shear stresses and surface tension temperature gradients on the free surface of fluid 1 were the first shear stress boundary condition:

$$\frac{\mu}{N_1}\left[\varepsilon(w_{1z}-\varepsilon u_{1x})h_{1x}-\frac{1}{2}\varepsilon^2(u_{1y}+v_{1x})h_{1y}\right.$$
$$-\frac{1}{2}(u_{1z}+\varepsilon w_{1x})(1-\varepsilon^2h_{1x}^2)$$
$$\left.+\frac{1}{2}\varepsilon^2(\varepsilon w_{1y}+v_{1z})h_{1x}h_{1y}\right]=-\gamma_TMa(\varepsilon T_{1x}-\varepsilon h_{1x}T_{1z}).$$
$$\text{at } z=-d_w-h_1(x,y,t) \tag{23}$$

and the second shear stress boundary condition:

$$\frac{\mu}{N_1}\left[-\varepsilon h_{1y}\left(\varepsilon^3u_{1x}h_{1x}^2-\varepsilon v_{1y}\left(1+\varepsilon^2h_{1x}^2\right)+w_{1z}\right)\right.$$
$$-\frac{1}{2}\varepsilon^2\left(u_{1y}+v_{1x}\right)h_{1x}\left(\varepsilon^2h_{1y}^2-1-\varepsilon^2h_{1x}^2\right)$$
$$-\varepsilon^2\left(\varepsilon w_{1x}+u_{1z}\right)h_{1x}h_{1y}$$
$$\left.+\frac{1}{2}\left(\varepsilon w_{1y}+v_{1z}\right)\left(1+\varepsilon^2h_{1x}^2-\varepsilon^2h_{1y}^2\right)\right]$$
$$=-\frac{\gamma_TMa}{N_1}\left[\varepsilon^3T_{1x}h_{1x}h_{1y}-\varepsilon T_{1y}\left(1+\varepsilon^2h_{1x}^2\right)+\varepsilon T_{1z}h_{1y}\right].$$
$$\text{at } z=-d_w-h_1(x,y,t) \tag{24}$$

where the ratio is defined as $\gamma_T = (d\gamma_1/dT)/(d\gamma_2/dT)$. The kinematic boundary condition of fluid 1 was

$$\varepsilon^2h_{1t}+\varepsilon u_1h_{1x}+\varepsilon v_1h_{1y}-w_1=0. \qquad \text{at } z=-d_w-h_1(x,y,t) \tag{25}$$

The boundary conditions of the temperature of fluid 1 and the wall were the following. At the wall

$$T_w=T_1 \qquad \text{and } \frac{\chi}{K}T_{wz}=T_{1z}. \qquad \text{at } z=-d_w \tag{26}$$

and at the free surface

$$\frac{1}{N_1}\left(-\varepsilon h_{1x}T_{1x}-\varepsilon h_{1y}T_{1y}+T_{1z}\right)=\frac{Bi_1}{d}\left(T_1-1\right).$$
$$\text{at } z=-d_w-h_1(x,y,t) \tag{27}$$

where $K = K_1/K_2$ and $\mathrm{Bi}_1 = Q_{h1}d_1/K_1$ is the Biot number of fluid 1 and Q_{h1} is the heat transfer coefficient at the interface of fluid 1.

As can be seen in the equations and boundary conditions presented above, their terms present different powers of ε. That difference plays an important role in the lubrication

approximation (Oron et al. 1997). The reason is that it is possible to obtain linear differential equations at each order of ε after substitution of Eqs. 1 and 2. Equations obtained at higher orders of ε include inhomogeneities which are derived from solutions of equations obtained at lower orders. The same method was applied to the corresponding boundary conditions.

With the boundary conditions it was possible to calculate the temperatures and pressures of the system at the lowest order in the lubrication approximation. Then, at the lowest order, the pressures of fluid 2 and fluid 1 were

$$p_0 = P_U - S\nabla_\perp^2 h \tag{28}$$

$$p_{10} = P_L - \gamma S\nabla_\perp^2 h_1 \tag{29}$$

where $\nabla_\perp^2 = \partial^2/\partial x^2 + \partial^2/\partial y^2$. The pressures P_U and P_L are different because they come from different atmospheres. They are uniform in space and therefore will not appear in the final evolution equations given below. As explained above, in the lubrication approximation only the pressures in Eqs. 28 and 29 are required and for that reason there is no need to expand S in terms of ε. At the lowest order the temperatures of fluid 2, wall and fluid 1 were:

$$T_{20}(z) = \frac{1}{den}\left[1 - Bi(z-h)\right] \tag{30}$$

$$T_{w0}(z) = \frac{1}{den}\left[1 - \frac{Bi}{\chi}(z - \chi h)\right] \tag{31}$$

$$T_{10}(z) = \frac{1}{den}\left[1 - \frac{Bi}{K}\left(z + d_w - K\left(\frac{d_w}{\chi} + h\right)\right)\right] \tag{32}$$

where the denominator was defined as

$$den = Bi\left(h + \frac{h_1}{K} + \frac{d_w}{\chi}\right) + 1 + \frac{d}{K}\frac{Bi}{Bi_1} \tag{33}$$

Notice in Eq. 32 that the temperature of fluid 1 in fact satisfied the boundary conditions even though Bi and h appear in its expression. It should be remembered that h_1 and Bi_1 appear in the denominator den Eq. 33 and that it was possible to satisfy the free surface boundary condition Eq. 27 and all the others. The same can be said about the solution of the temperaure of the wall Eq. 31. It is important to point out here the relevance of the denominator den which is the thermal interaction factor between the two fluids in the evolution equations of the two free surface perturbations taking into account that the denominator den is a function of x, y and t through the free surface deformations $h(x, y, t)$ and $h_1(x, y, t)$.

Notice that the procedure only needs solutions up to the first order in the approximation. For that reason, there is no need to expand in terms of ε the Marangoni number Ma which first appears at first order. The following nonlinear evolution equations are obtained for the free surface deformations of fluid 2 and fluid 1. Therefore,

$$h_t + \frac{1}{3}S\nabla_\perp\cdot\left[h^3\nabla_\perp\left(\nabla_\perp^2 h\right)\right] - Ma\nabla_\perp\cdot\left[h^2\nabla_\perp\left(\frac{1}{den}\right)\right] = 0. \tag{34}$$

and

$$h_{1t} + \frac{1}{3}\frac{\gamma S}{\mu}\nabla_\perp\cdot\left[h_1^3\nabla_\perp\left(\nabla_\perp^2 h_1\right)\right] + Ma\frac{\gamma_T}{\mu}\frac{d}{K}\frac{Bi}{Bi_1}\nabla_\perp \cdot\left[h_1^2\nabla_\perp\left(\frac{1}{den}\right)\right] = 0. \tag{35}$$

The Eqs. 34 and 35 have a symmetric presentation.

In what follows a discussion is given about the minus sign in front of Ma in Eq. 34 and the plus sign in front of the Ma in Eq. 35. In Eq. 34 the minus sign seems to be destabilizing but expanding the spatial derivatives, terms with minus and plus sign appeared. The term with minus sign appeared in the linear theory. The plus sign in the Ma term in Eq. 35 seems to be stabilizing (it is well known that this is the case if fluid 2 was absent). However, the sign in front of each term can be decided only after expanding completely the spatial derivatives of different orders of den. Some terms of Ma were negative and other terms had positive signs. The one which appeared in the linear theory was positive. In this way, the thermal coupling between the two fluids through the wall is able to destabilize the whole system by means of the coupled nonlinear evolution Eqs. 34 and 35.

Those coupled Eqs. 34 and 35 reduce to one in the limit when the relative thickness of fluid 1 tends to zero, that is d $\to$ 0. In this limit, $h_1 = d + H_1 \to 0$ because the perturbation H_1 should be zero when there is no fluid layer. The denominator shows no coupling and reduces to $den =$ Bi $(h + d_w/\chi) + 1$ (see Kabova et al. 2006 and Dávalos-Orozco 2012). Notice that the limit $\chi \to \infty$ only has effect in the denominator "den", the place where it appears. In previous papers (Dávalos-Orozco 2012, 2014, 2015, 2016), which included the thickness of the wall, this limit is equivalent to making zero the ratio d_w/χ which corresponds to a wall of zero thickness, therefore heat is conducted very well. This is why that ratio is written explicitly in den. The other terms in den show the influence the ratio of the heat conductivity of the fluids has on the thermal interaction and consequently on the instability.

Linear Stability

Equations 34 and 35 have been linearized to understand the instability of the coupled fluid layers. A normal mode

separation of variables was assumed for the amplitudes of free surface deformations of the two fluids. They are:

$$H(x,y,t) = A\exp\left[i\left(k_x x + k_y y\right) + \Omega t\right]. \tag{36}$$

$$H_1(x,y,t) = B\exp\left[i\left(k_x x + k_y y\right) + \Omega t\right] \tag{37}$$

where $\Omega = \Gamma + i\omega$, Γ is the growth rate and ω is the frequency of oscillation of the perturbations. The following system of algebraic equations is obtained after substitution:

$$\left[\frac{\Omega}{k^2} + \frac{1}{3}Sk^2 - \left(\frac{MaBi}{den_L^2}\right)\right]A - \frac{1}{K}\left(\frac{MaBi}{den_L^2}\right)B = 0 \tag{38}$$

from Eq. 34 and

$$\left(\frac{MaBi}{den_L^2}\right)\frac{\gamma_T}{\mu}\frac{d^3}{K}\frac{Bi}{Bi_1}A + \left[\frac{\Omega}{k^2} + \frac{1}{3}\frac{\gamma d^3}{\mu}Sk^2 + \left(\frac{MaBi}{den_L^2}\right)\frac{\gamma_T}{\mu}\frac{d^3}{K^2}\frac{Bi}{Bi_1}\right]B = 0 \tag{39}$$

from Eq. 35, where $k^2 = k_x^2 + k_y^2$ and

$$den_L = Bi\left(1 + \frac{d}{K} + \frac{d_w}{\chi}\right) + 1 + \frac{d}{K}\frac{Bi}{Bi_1} \tag{40}$$

appears due to the linearization of $1/den$ and its powers (see Eq. 33).

The solvability condition of the system of Eqs. 38 and 39 is its determinant zero:

$$\left[\frac{\Omega}{k^2} + \frac{1}{3}Sk^2 - \left(\frac{MaBi}{den_L^2}\right)\right]\times\left[\frac{\Omega}{k^2} + \frac{1}{3}\frac{\gamma d^3}{\mu}Sk^2 + \left(\frac{MaBi}{den_L^2}\right)\frac{\gamma_T}{\mu}\frac{d^3}{K^2}\frac{Bi}{Bi_1}\right] + \left(\frac{MaBi}{den_L^2}\right)^2\frac{\gamma_T}{\mu}\frac{d^3}{K^2}\frac{Bi}{Bi_1} = 0 \tag{41}$$

which gives a quadratic equation for Ω. The two solutions have a radical. If the radicand is positive the solutions are real and the growth rate can be positive (instability grows with time), zero (criticality) or negative (stable perturbation which decreases in time). If the radicand is negative, Ω is complex and the imaginary part is the frequency of oscillation of a perturbation which grows in time if the real part is positive or decreases in time if the real part is negative.

The number of parameters is too large. Then from now on it is assumed in the linear and nonlinear problem that fluid 2 and fluid 1 are the same and that the atmospheres outside them have the same physical properties but with different temperatures as shown in Fig. 1. In that case, the following parameters are fixed: $\alpha = \mu = \gamma = \gamma_T = K = 1$ and $Bi_1 = Bid$. Even under these simplifications the system is very complex. However, in the linear problem it is not necessary to fix S and Bi because the solutions to Eq. 41 can be written as:

$$\Omega_p = \frac{1}{2}k^2\left\{-\left[k^2\left(d^3+1\right) + A_p\left(d^2-1\right)\right] \pm\left[k^4\left(d^3-1\right)^2 + 2A_pk^2\left(d^3-1\right)\left(d^2+1\right) + A_p^2\left(d^2-1\right)^2\right]^{\frac{1}{2}}\right\} \tag{42}$$

Here $\Omega_p = \Omega/(S/3) = \Gamma_p + i\omega_p$ and

$$A_p = \frac{3MaBi}{Sden^2} \tag{43}$$

The solution with the plus sign is called the first solution and that with the minus sign is called the second solution. Notice that the flow is stable when $d = 1$. It is found that the stability has different results when $d > 1$ from when $d < 1$. This difference is made clear with some exact and approximate analytical results found from Eq. 42. If the flow is stationary, the critical wavenumber k_C was found to be

$$k_{CS}^2 = A_{pCS}\frac{d-1}{d} \tag{44}$$

Notice that there is only one root. Clearly, from this result, it is not possible to have a critical wavenumber for stationary convection if $A_{pC} > 0$ and $d < 1$ or else, if $A_{pC} < 0$ and $d > 1$. This will have important consequences in the results presented below. The approximate wave number of the maximum growth rate for stationary convection was

$$k_{maxstat}^2 = A_{pmaxstat}\left(\frac{d^2 - 3d - 3 + \sqrt{d^4 + 10d^3 + 19d^2 + 18d + 9}}{4\left(d^2 + d + 1\right)}\right) \tag{45}$$

which is a good approximation for $d > 2$ and $A_{pmaxstat} > 0$.

Now a discussion is given for the solutions with $d < 1$. In this case stationary and oscillatory convection are possible. In the stationary case, when the radicand is positive in the solutions Eq. 42 of Ω, there is no critical wavenumber. The reason is that the first and second solutions merge for a finite value of Γ_p and the stationary curve never touches the k axis ($\Gamma_p = 0$). Besides, the second mode of the first solution found after the last wavenumber of oscillatory convection (see below) is always stable. However it is possible to calculate an approximate wavenumber corresponding to the maximum growth rate. It was found as

$$k^2_{maxstatd<1} = \frac{A_{maxstatd<1}}{12}\left[10 - \left(r_m + \frac{1}{r_m}\right) + i\sqrt{3}\left(r_m - \frac{1}{r_m}\right)\right] \tag{46}$$

where

$$r_m = \sqrt[3]{-1 - 54d + 6d\sqrt{3 + 81d^2}} \tag{47}$$

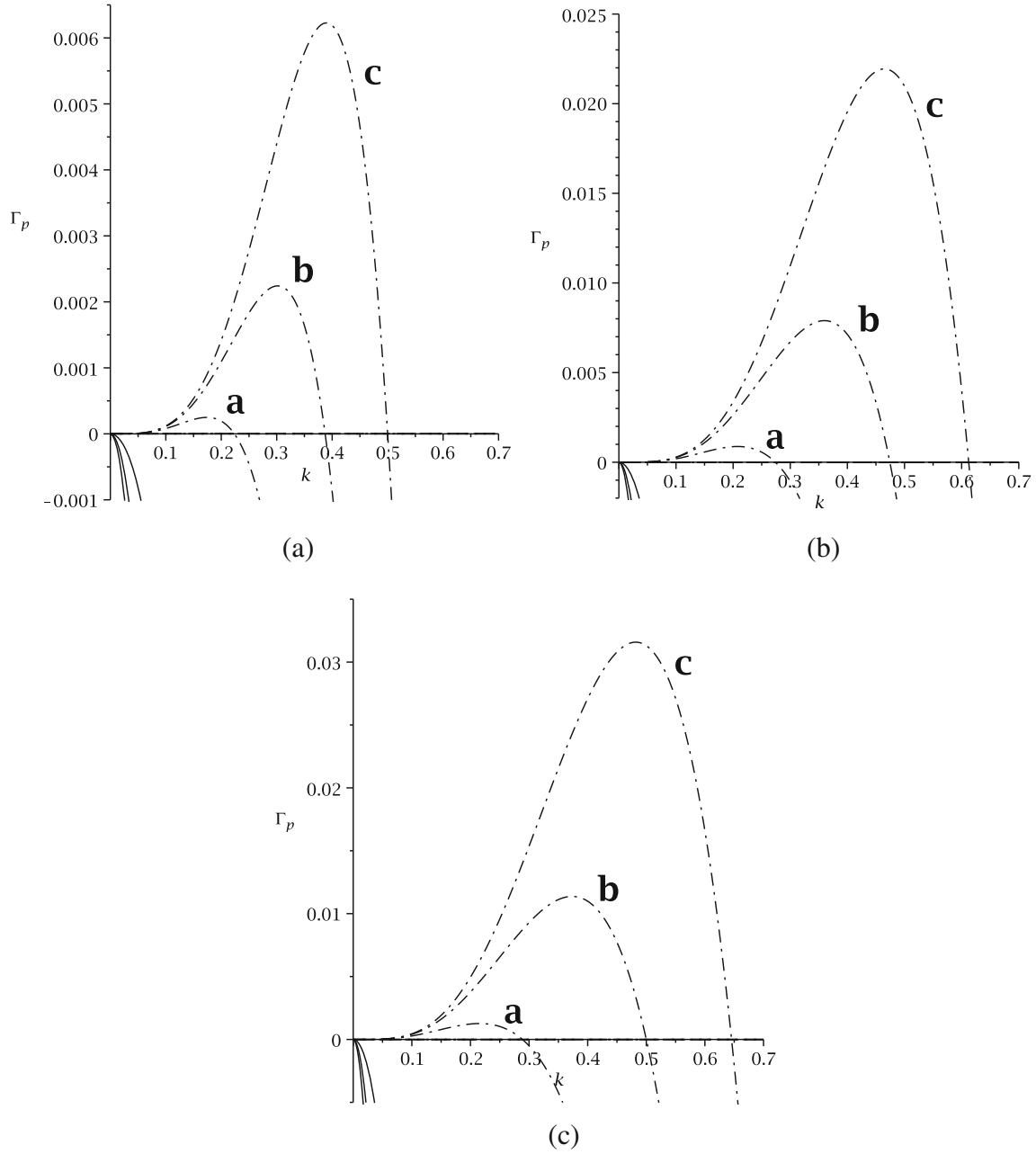

Fig. 2 Γ_p vs k. Only stationary convection (first solution, dashdotted line) for $d > 1$. There exists a critical Marangoni number Ma_C ($\Gamma_p = 0$). The second solution (solid line) of Γ_p is always stable. **a** $d = 2$, **b** $d = 4$, **c** $d = 6$. **a** $A_p = 0.1$, **b** $A_p = 0.3$ and **c** $A_p = 0.5$

Notice that $k^2_{maxstatd<1}$ is a complex number. However, when taking the square root the imaginary part gives a value of the order 10^{-11}. The formula is good up to $A_p = 0.5$.

Now, when $d < 1$ and the radicand in Eq. 42 is negative, it is possible to have oscillatory convection. The wavenumber k^2_{CO1} after which oscillations start to appear was

$$k^2_{CO1} = A_{pCO1}\frac{1-d}{d^2+d+1} \tag{48}$$

This is also the location where the first and second solutions of Ω merge to change into oscillatory flow. The wavenumber k^2_{CO2} where oscillations end was

$$k^2_{CO2} = A_{pCO2}\frac{(d+1)^2}{d^3-1} \tag{49}$$

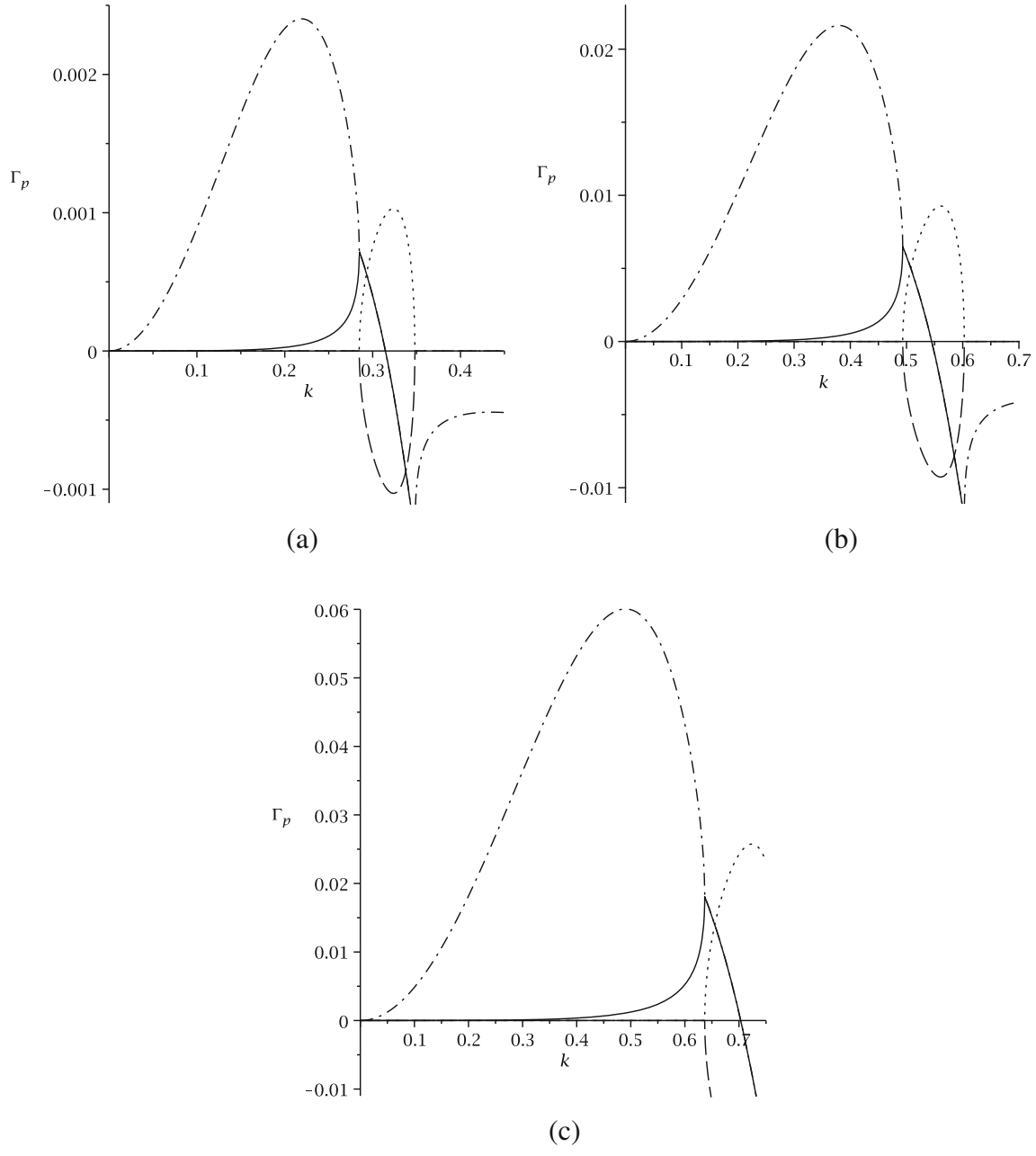

Fig. 3 Scaled Γ_p vs k. Stationary and oscillatory convection for $d < 1$. $d = 0.1$ and **a** $Ap = 0.1$, **b** $Ap = 0.3$, **c** $Ap = 0.5$. dash-dotted lines are the first and second mode of the first solution of Γ_p. The second mode is never unstable. The solid line corresponds to the second solution of Γ_p. Both solutions merge into one (solid line) at the wavenumber where oscillatory convection begins. There is a critical Marangoni number Ma_C for oscillatory convection. Above the critical wavenumber k_C, oscillatory and then stationary convection remain stable. The dotted and dashed lines correspond to the frequencies of oscillation ω_p

Between these two k's the growth rate decreases to $\Gamma_p = 0$ at the following critical k_{CO}^2 of oscillatory convection

$$k_{CO}^2 = A_{pCO}\frac{1-d}{d^2-d+1} \tag{50}$$

They (Eqs. 48 to 50) are only valid for $A_{pC} > 0$ and $d < 1$ or else for $A_{pC} < 0$ and $d > 1$. Therefore, not all the k range of oscillatory convection is unstable. The maximum frequency of unstable convection occurs when k^2 approaches to k_{CO}^2, (near $\Gamma_p = 0$) where its value was

$$\omega_p = A_p^2\frac{d\,(1-d)^2}{\left(d^2-d+1\right)^2}\sqrt{d^2+1} \tag{51}$$

However, the absolute maximum frequency of oscillation occurs at

$$k_{\omega_p max}^2 = \frac{A_p}{4}\left(\frac{3\left(d^2+1\right)+\sqrt{d^4+34d^2+1}}{(1-d)\left(d^2+d+1\right)}\right) \tag{52}$$

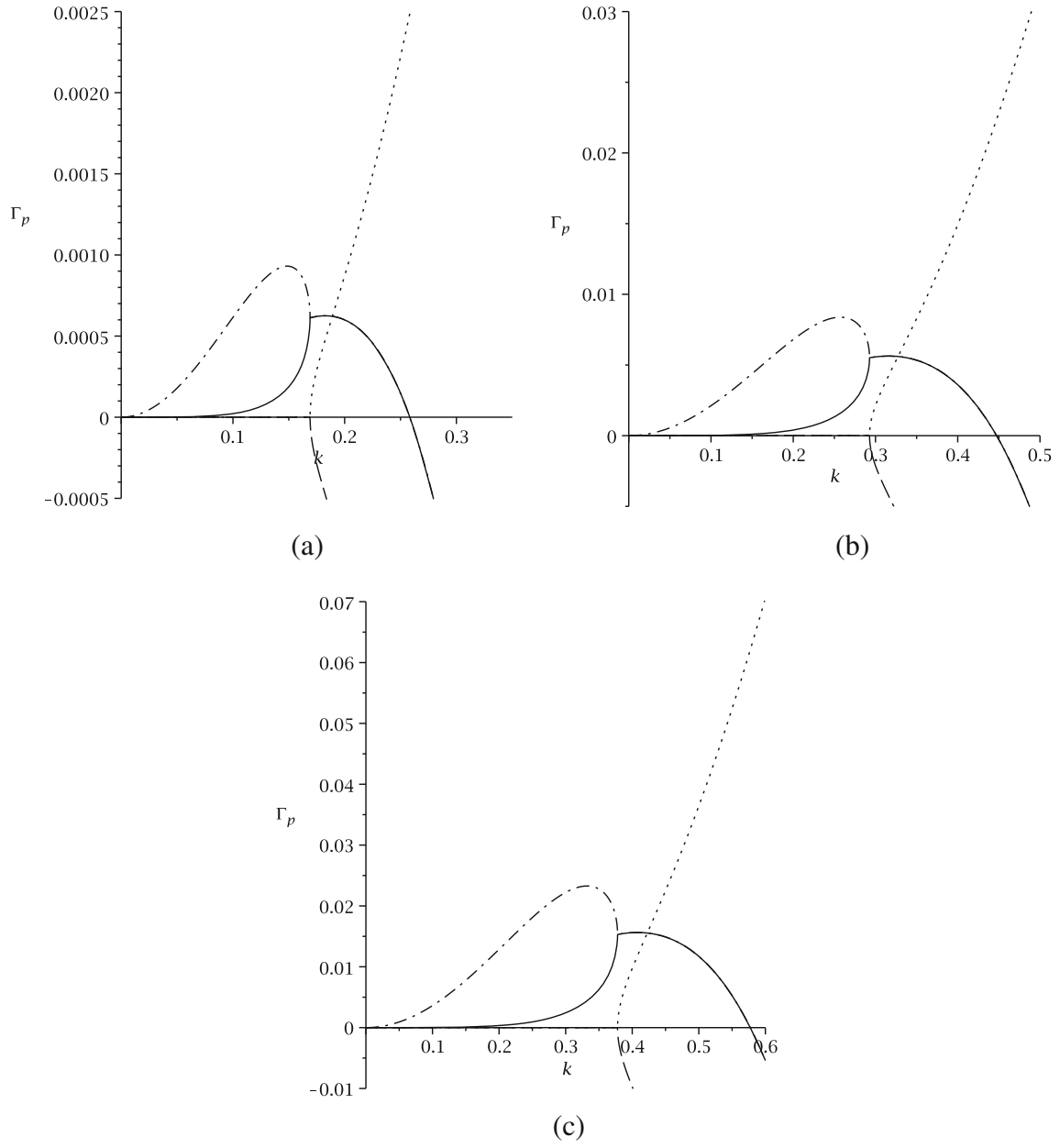

Fig. 4 Scaled Γ_p vs k. Stationary and oscillatory convection for $d < 1$. $d = 0.5$ and **a** $Ap = 0.1$, **b** $Ap = 0.3$, **c** $Ap = 0.5$. dash-dotted lines are the first and second mode (not shown) of the first solution of Γ_p. The second mode is never unstable. The solid line corresponds to the second solution of Γ_p. Both solutions merge into one (solid line) at the wavenumber where oscillatory convection begins. There is a critical Marangoni number Ma_C for oscillatory convection. Above the critical wavenumber k_C, oscillatory and then stationary convection remain stable. The dotted and dashed lines correspond to the frequencies of oscillation ω_p

which is always located after the critical, that is $k^2_{CO} < k^2_{\omega_p max}$. It is stable and is of no interest here. Moreover, it is interesting that under particular conditions the growth rate of unstable oscillatory convection may have a maximum at

$$k^2_{\Gamma_p max O} = \frac{A_{\Gamma_p max O}}{2} \frac{1-d}{d^2-d+1} \tag{53}$$

In other words, when it exists, it occurs between k^2_{CO1} and k^2_{CO}. The condition Γ_p has to satisfy to have a maximum is that $k^2_{\Gamma_p max O} > k^2_{CO1}$. This happens when d satisfies $1 > d > (3-\sqrt{5})/2$. Below this magnitude the growth rate decreases monotonically with k and the the maximum of Γ_p appears at k^2_{CO1}, the first wavenumber for oscillatory convection.

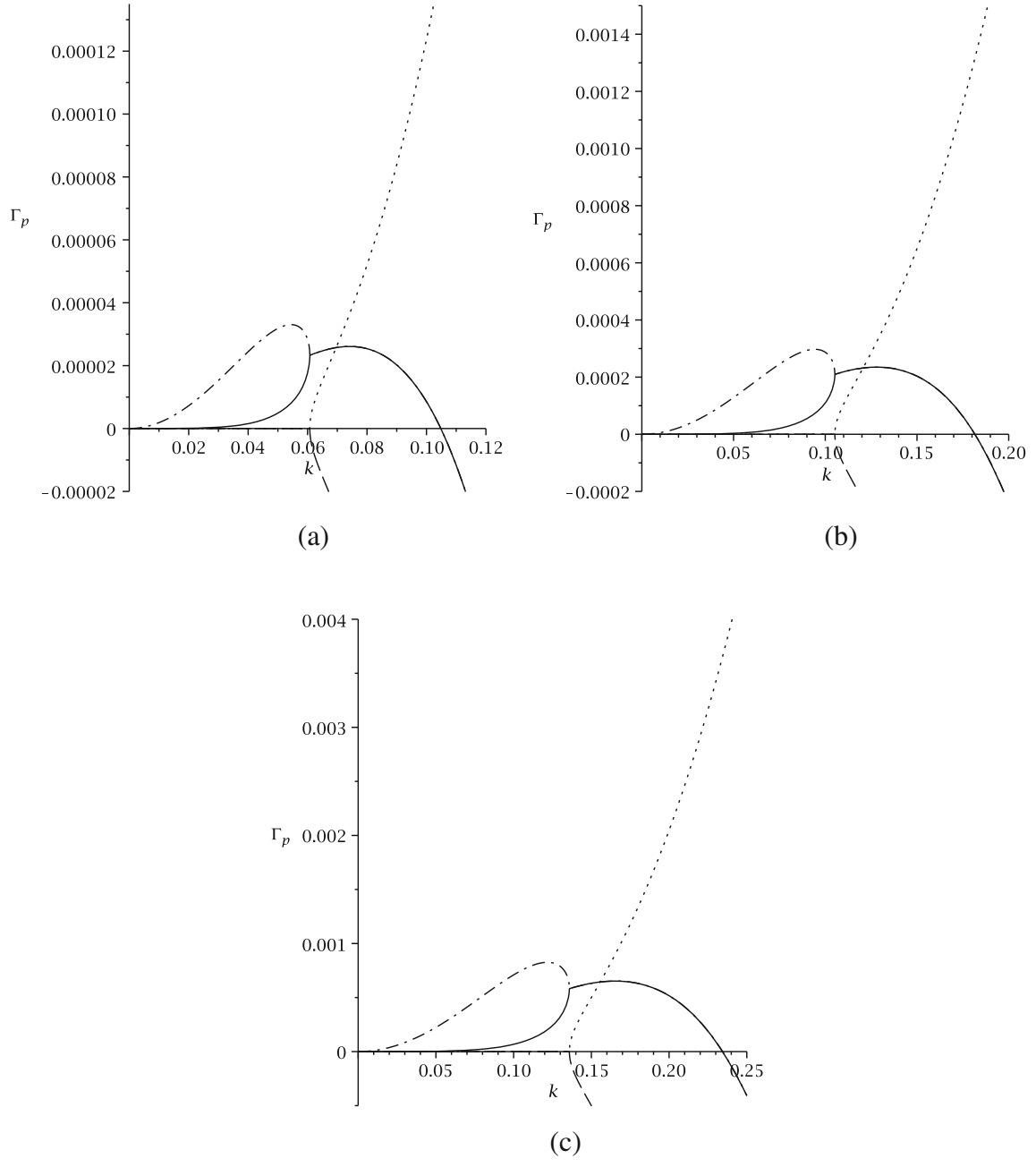

Fig. 5 Scaled Γ_p vs k. Stationary and oscillatory convection for $d < 1$. $d = 0.9$ and **a** $Ap = 0.1$, **b** $Ap = 0.3$, **c** $Ap = 0.5$. dash-dotted lines are the first and second mode (not shown) of the first solution of Γ_p. The second mode is never unstable. The solid line corresponds to the second solution of Γ_p. Both solutions merge into one (solid line) at the wavenumber where oscillatory convection begins. There is a critical Marangoni number Ma_C for oscillatory convection. Above the critical wavenumber k_C, oscillatory and then stationary convection remain stable. The dotted and dashed lines correspond to the frequencies of oscillation ω_p

From the results presented above it is concluded that the stability is determined by two sets of conditions. The first set is $A_p > 0$ and $d > 1$ (stationary convection) or else, $A_p > 0$ and $d < 1$ (stationary convection and oscillatory convection). The second set is $A_p < 0$ and $d < 1$ (stationary convection) or else, $A_p < 0$ and $d > 1$ (stationary convection and oscillatory convection). In the results presented below, the first set of conditions was used.

The linear problem was described by means of plots of the growth rate Γ_p against the wavenumber. With them the analytical results were clarified. In Figs. 2, 3, 4 and 5 the parameters d and A_p were varied to understand the behaviour of the growth rate. In all the graphics of the linear problem the first solution for Γ_p was plotted with dashdotted lines, the second solution with solid lines, the frequency of the first solution with dotted lines and the frequency of the second solution with dashed lines. Figure 2 presents sample results for $d > 1$. In this case only stationary convection is possible and a critical wave number was found as in Eq. 44. As can be seen, $k = 0$ is also

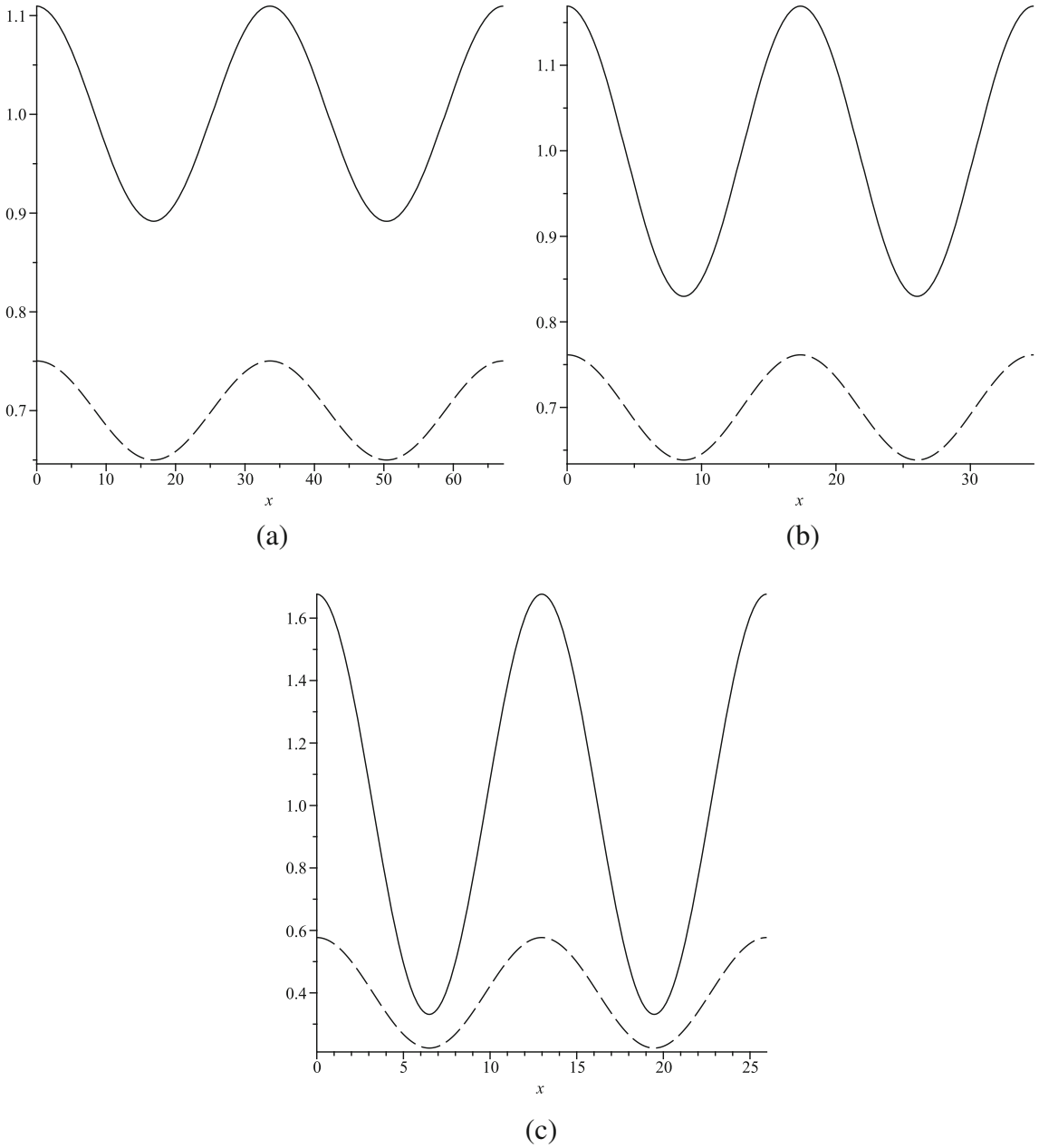

Fig. 6 Nonlinear mode: $d > 1$. Stationary convection. $d_w/\chi = 0.1$. **a** $d = 2$, $Ma = 1.8$ ($A_p \approx 0.1$), $k = 0.187$, t = 200, Sinuous. **b** $d = 4$, $Ma = 6.3$ ($A_p \approx 0.3$), $k = 0.362$, t = 200, Sinuous. **c** $d = 6$, $Ma = 12.3$ ($A_p \approx 0.5$), $k = 0.484$, t = 200, Sinuous. Notice that they were sinuous for both ($A_1(0) = A_1^*(0) = 0.05$ and $B_1(0) = B_1^*(0) = 0$) and ($A_1(0) = A_1^*(0) = 0$ and $B_1(0) = B_1^*(0) = 0.05$)

a critical wavenumber. The magnitudes of d were $d = 2$ (Fig. 2a), $d = 4$ (Fig. 2b) and $d = 6$ (Fig. 2c). In each figure A_p varies as a) $A_p = 0.1$, b) $A_p = 0.3$, c) $A_p = 0.5$. Clearly, the growth rate increases with A_p which is proportional to the Marangoni number. Besides, the increase of d, from Fig. 2a to c, also has an important contribution to increase the growth rate. An approximate wavenumber for the maximum growth rate for stationary convection is given in Eq. 45.

The linear results of $d < 1$ were presented in Figs. 3 to 5. Figure 3 corresponds to $d = 0.1$. The dotdashed line corresponds to the first solution of Γ_p and the solid line corresponds to the second solution. Due to the number of details of the stability, the curves were presented in three different graphs. The results for $A_p = 0.1$ were shown in Fig. 3a, for $A_p = 0.3$ in Fig. 3b and for $A_p = 0.5$ in Fig. 3c. The range of the wavenumber is limited to $k < 0.7$ in order to include the relevant results to k around 0.5. In

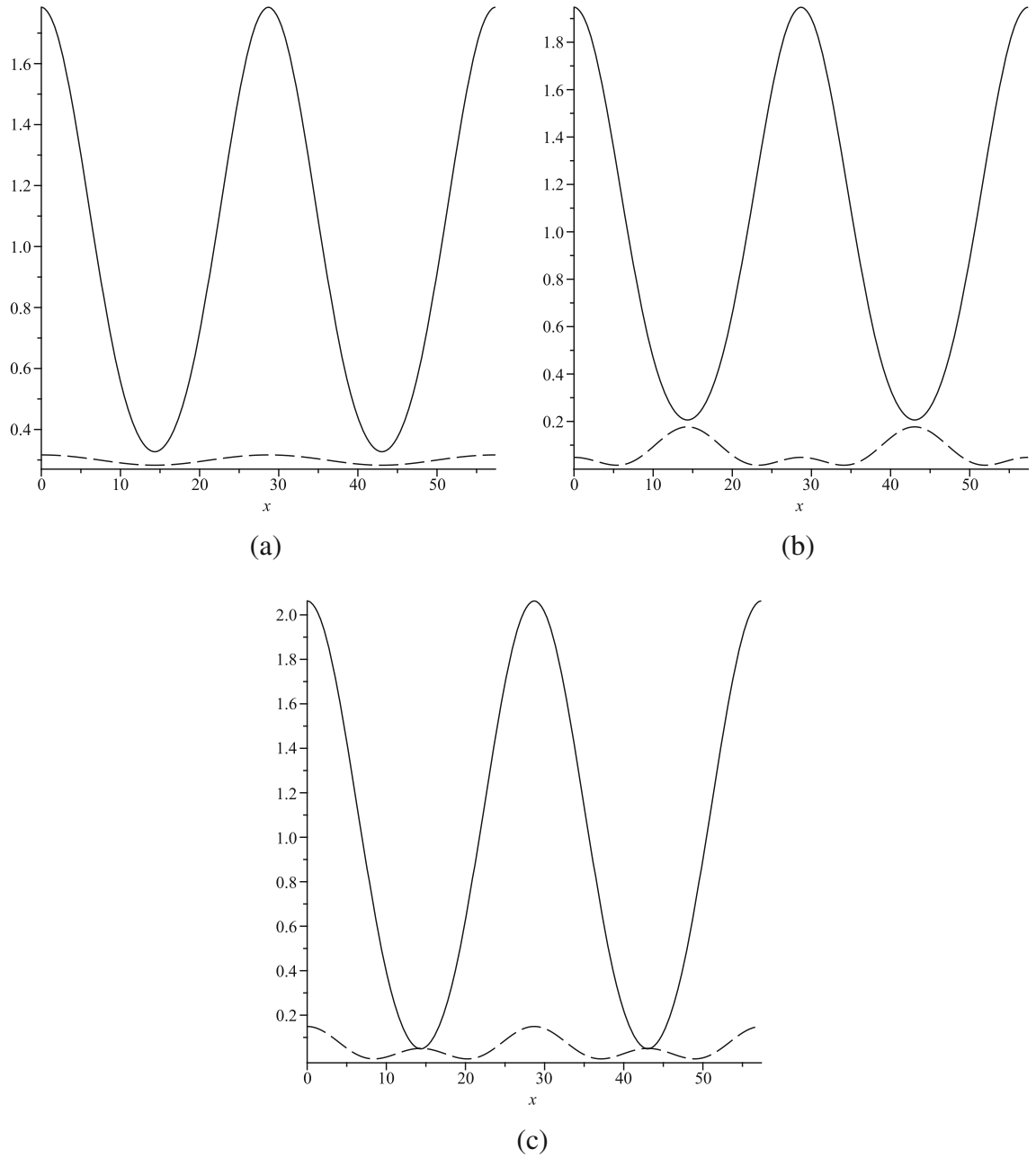

Fig. 7 Nonlinear mode: $d < 1$. Stationary convection. $d_w/\chi = 0.1$, $d = 0.1$, $Ma = 1.5$ ($A_p \approx 0.1$), $k = 0.219$. **a** $A_1(0) = A_1^*(0) = 0.05$, t = 3000, Sinuous. **b** $B_1(0) = B_1^*(0) = 0.05$, t = 3000, Varicose. **c** $B_1(0) = B_1^*(0) = 0.05$, t = 7500, Sinuous

Fig. 3a and b it is possible to observe the second stationary mode of the first solution of Γ_p for $k > 0.35$ in Fig. 3a and $k > 0.6$ in Fig. 3b. The fact that this mode is always stable has as a consequence that no critical wavenumber exists when $d < 1$. For this reason and for the sake of presentation, this stable second stationary mode was not presented in the following figures. In Fig. 3 the two solutions merge into one curve at the point k^2_{CO1} where oscillatory convection starts. Only Fig. 3a and b show the end of oscillatory convection at k^2_{CO2}, point after which the second stationary mode appears. The critical wavenumber k^2_{CO} of oscillatory convection is located at the point where the solid curve touches the k axis and $\Gamma_p = 0$. The increase of A_p increases the growth rate of stationary convection. Moreover, it also increases the magnitude of the Γ_p where the two solutions merge to start oscillatory convection. Notice that the frequency of oscillation increases too in the unstable range, to the left of k^2_{CO}.

The following figures present similar characteristics. In Fig. 4 results were presented for $d = 0.5$. It is

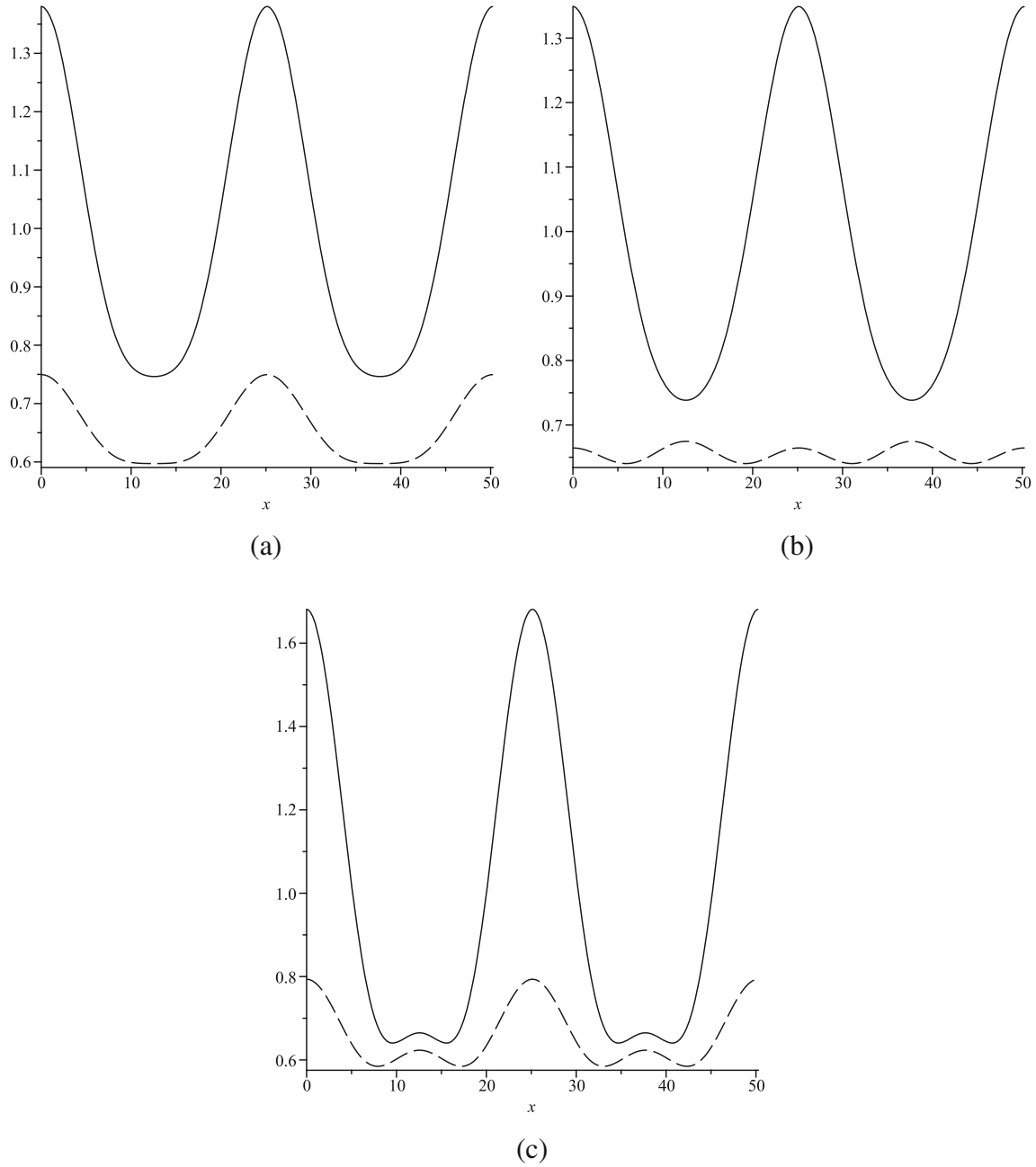

Fig. 8 Nonlinear mode: $d < 1$. Stationary convection. $d_w/\chi = 0.1$, $d = 0.5$, $Ma = 4.7$ ($A_p \approx 0.3$), $k = 0.25$. **a** $A_1(0) = A_1^*(0) = 0.05$, t = 300, Sinuous. **b** $B_1(0) = B_1^*(0) = 0.05$, t = 300, Varicose. **c** $B_1(0) = B_1^*(0) = 0.05$, t = 450, Sinuous

interesting that the growth rate decreases in all the range of k considered. However, the frequency of oscillatory convection increases notably in the unstable k range of the stability. The wave numbers where oscillatory convection begins k^2_{CO1} (Eq. 48) and that corresponding to the critical k^2_{CO} (Eq. 50) decrease their magnitude. However, A_p contributes to increase their magnitude as seen from Fig. 4a to c.

In Fig. 5 the magnitude of d is increased to $d = 0.9$. This reduces considerably the growth rate in all the range of k. The magnitudes of k^2_{CO1} (Eq. 48) and k^2_{CO} (Eq. 50) are decreased further, in such a way that there is only a very small wavenumber range of instability. It is interesting that the unstable frequency has a decrease for this d in comparison with the previous Figs. 3 and 4. In fact, the maximum of unstable frequency Eq. 51, near $\Gamma_p = 0$ has also a maximum with respect to d. That maximum was found to correspond to

$$d_{max\,freq} = \frac{1}{6}\left[\left(4\sqrt{113}+36\right)^{\frac{1}{3}} - \left(4\sqrt{113}-36\right)^{\frac{1}{3}}\right] \tag{54}$$

which is approximately $d_{max\,freq} = 0.4023199$. The results of Fig. 4 were near to this $d_{max\,freq}$ and therefore had an increase in unstable frequency. Those of Fig. 5 are far from this $d_{max\,freq}$ and the frequency decreased even below that of Fig. 3. In contrast, it was shown that the maximum of the growth rate of oscillatory convection decreases monotonically from $d = 0$ to $d = 1$ (where the flow is already stable, see Eq. 42).

The subject of the next section is the nonlinear problem. The interest is to find out which mode, the sinuous or the varicose, will prevail in the instability.

Nonlinear Sinuous and Varicose Modes of Instability

Here numerical analysis is made of the coupled nonlinear Eqs. 34 and 35 under the same assumption of the previous section, that is, the fluids and the atmospheres outside them were the same but with different temperatures.

The analysis of the free surface deformations h and h_1 in Eqs. 34 and 35 was made by means of a three-term expansion using the first two normal modes. They are

$$h = 1 + A_1(t)e^{ikx} + A_2(t)e^{2ikx} + c.c. \tag{55}$$

$$h_1 = d + B_1(t)e^{ikx} + B_2(t)e^{2ikx} + c.c. \tag{56}$$

where c.c. means complex conjugate. These expressions were substituted in Eqs. 34 and 35 to obtain a set of time nonlinear ordinary differential equations for the coefficients. Substitution was made of $\alpha = \mu = \gamma = \gamma_T = K = 1$, $Bi_1 = Bid$ with $S = 1$ and $Bi = 0.1$. Now, assuming that an asterisk means complex conjugate, the equations have the form:

$$\begin{aligned}
&\frac{dA_1}{dt} + k^4\left(\frac{1}{3}A_1 + A_1^2A_1^* + 7A_2A_1^*\right)\\
&+\frac{Mak^2}{10den^2}\Big[-\Big(A_1 + B_1 + 2A_1^*A_2 + A_1^2A_1^* - 2B_1^*A_2\\
&\quad +4B_2A_1^* - A_1^2B_1^* + 2A_1B_1A_1^*\Big)\\
&\quad +\frac{1}{10den}\Big(2A_1^*A_2 + 4B_1^2A_1^* + 2B_1^*A_2 + 4A_1^2A_1^*\\
&\quad +8A_1B_1A_1^* + 2A_1^*B_2 + 2B_1^*B_2\Big)\\
&\quad -\frac{3}{100den^2}\Big(A_1^*A_1^2 + A_1^2B_1^* + B_1^2B_1^* + A_1^*B_1^2\\
&\quad +2A_1^*B_1A_1 + 2A_1B_1B_1^*\Big)\Big] = 0
\end{aligned} \tag{57}$$

$$\begin{aligned}
&\frac{dA_2}{dt} + k^4\left(\frac{16}{3}A_2 + 2A_1^2\right)\\
&+\frac{2Mak^2}{5den^2}\Big[-\Big(A_2 + B_2 + A_1^2 + B_1A_1\Big)\\
&+\frac{1}{10den}\Big(B_1^2 + 2B_1A_1 + A_1^2\Big)\Big] = 0
\end{aligned} \tag{58}$$

$$\begin{aligned}
&\frac{dB_1}{dt} + k^4d\left(\frac{d^2}{3}B_1 + B_1^2B_1^* + 7dB_1^*B_2\right) + \frac{Mak^2}{5den^2}\\
&\Big[\Big(\frac{d^2}{2}(A_1 + B_1) - dB_2A_1^* + 2dB_1^*A_2 + dB_1^*B_2\\
&+B_1A_1B_1^* - \frac{1}{2}B_1^2A_1^* + \frac{1}{2}B_1^2B_1^*\Big)\\
&-\frac{d}{5den}\Big(A_1^2B_1^* + B_1^2B_1^* + 2A_1B_1B_1^*\\
&+\frac{d}{2}\left(B_1^*A_2 + A_1^*A_2 + B_2A_1^* + B_1^*B_2\right)\Big)\\
&+\frac{3d^2}{200den^2}\Big(B_1^2A_1^* + A_1^*A_1^2 + B_1^2B_1^*\\
&+2A_1B_1A_1^* + A_1^2B_1^* + 2A_1B_1B_1^*\Big)\Big] = 0
\end{aligned} \tag{59}$$

$$\begin{aligned}
&\frac{dB_2}{dt} + 2k^4d^2\left(\frac{8}{3}dB_2 + B_1^2\right)\\
&+\frac{2dMak^2}{5den^2}\Big[B_1^2 + B_1A_1 + dA_2 + dB_2\\
&-\frac{d}{den}\left(\frac{1}{10}A_1^2 + \frac{1}{10}B_1^2 + \frac{1}{5}A_1B_1\right)\Big] = 0
\end{aligned} \tag{60}$$

The complex conjugate equations also form part of the complete set of eight coupled nonlinear ordinary differential

equations. They were solved using the package Maple. For initial value problems it uses a Runge-Kutta Fehlberg method (rkf45) that produces a fifth order accurate solution. The numerical solution was done assuming two kinds of initial perturbations. First, the perturbations were applied at the free surface of fluid 2 and $A_1(0) = A_1^*(0)$ are given with the other initial amplitudes zero. Second, the perturbations were applied at the free surface of fluid 1 and $B_1(0) = B_1^*(0)$ were given with the other initial amplitudes zero. Here, $A_1^*(0)$ and $B_1^*(0)$ are the initial values of the complex conjugate amplitudes.

Sample figures were selected to present the nonlinear results. The parameters χ and d_w appear in the denominator den in one parameter d_w/χ. It is important to point out that increasing this ratio decreases the magnitude of the growth rate by diminishing the destabilizing effect of the Marangoni number.

This ratio d_w/χ was fixed in what follows because the principal goal was to approximate the parameter A_p to the magnitudes used in the linear problem. This was possible by fixing the required d and adjusting with the Marangoni number. The unstable wavenumber for

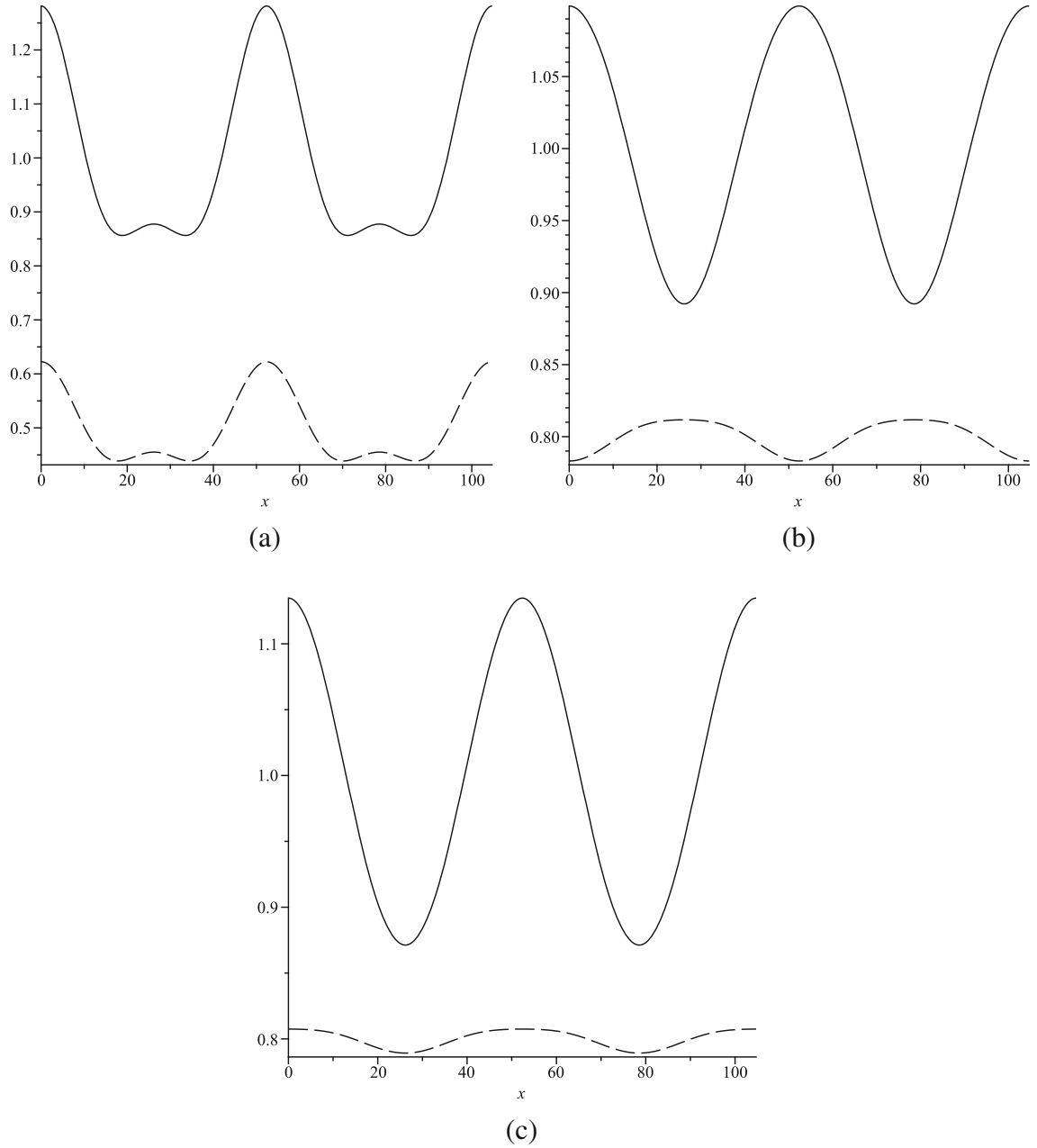

Fig. 9 Nonlinear mode: $d < 1$. Stationary convection. $d_w/\chi = 0.1$, $d = 0.9$, $Ma = 8.1$ ($A_p \approx 0.5$), $k = 0.12$. **a** $A_1(0) = A_1^*(0) = 0.05$, t = 400, Sinuous. **b** $B_1(0) = B_1^*(0) = 0.05$, t = 400, Varicose. **c** $B_1(0) = B_1^*(0) = 0.05$, t = 500, Sinuous

stationary convection used to understand which mode will prevail, sinuous or varicose, in the instability was selected as one close to that corresponding to the maximum growth rate. As discussed above, the growth rate of unstable oscillatory convection not always has a maximum. Therefore, the selected wavenumber was obtained applying the following calculation $\sqrt{\left(k_{CO1}^2 + k_{CO}^2\right)/2}$.

Computations were done for $A_p = 0.1$, 0.3 and 0.5 for each of the selected magnitudes of d. Notice that not all of those results were presented. This allowed us to have general conclusions related with the sample solutions presented in the next figures. The discussion of the nonlinear problem starts with $d > 1$. From the linear results it is known that only stationary convection can occur in this case. Figure 6 reviews the results of this case for $d = 2$ (Fig. 6a), $d = 4$ (Fig. 6b) and $d = 6$ (Fig. 6c). Each figure shows results for a selected A_p with a corresponding Ma. The wavenumbers were near to the maximum growth rate. It is found that, in all cases, the nonlinear mode of the perturbations is sinuous under the two initial conditions

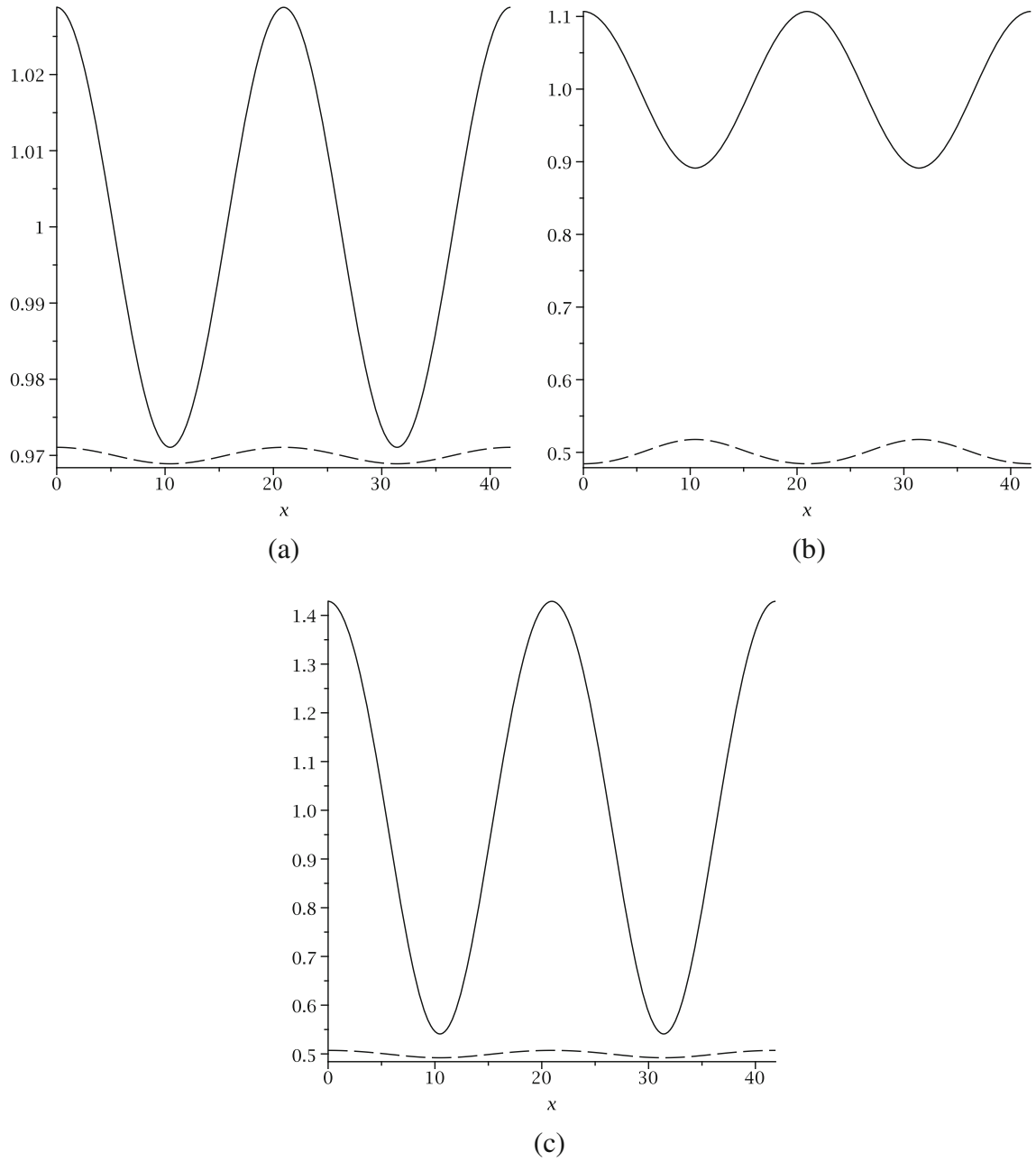

Fig. 10 Nonlinear mode: $d < 1$. Oscillatory convection. $d_w/\chi = 0.1$, $d = 0.1$, $Ma = 1.5$ ($A_p \approx 0.1$), $k = 0.30$, $\omega_p = 0.00075$. **a** $A_1(0) = A_1^*(0) = 0.01$, t = 1500, Sinuous. **b** $B_1(0) = B_1^*(0) = 0.01$, t = 1500, Varicose. **c** $B_1(0) = B_1^*(0) = 0.01$, t = 4500, Sinuous

considered. They are $A_1(0) = A_1^*(0) = 0.05$ (perturbations at the free surface of fluid 2) and $B_1(0) = B_1^*(0) = 0.05$ (perturbations at the free surface of fluid 1).

The results for of Fig. 6 are in contrast with those when $d < 1$. The solutions in this case were presented considering the magnitude of A_p in each figure. Figure 7 shows curves for stationary convection when $d = 0.1$ and $A_p \approx 0.1$. It is found that the nonlinear mode is always sinuous (Fig. 7a, t = 3000) when perturbations are applied to fluid 2. However, if the perturbations are applied to fluid 1 (Fig. 7b, t = 3000), it is possible to change the mode of instability to a varicose one. Nevertheless, this mode is able to change around time t = 7500 (Fig. 7c) into the sinuous mode. The sinuous mode, which seems to be the natural one for convection, remains for the full time of the calculation.

A similar behavior of stationary convection was found in Fig. 8 for $d = 0.5$ and $A_p \approx 0.3$ with $Ma = 4.7$. When the perturbation is applied to fluid 2 (Fig. 8a, t = 300) the nonlinear mode was sinuous all the time. However, application of the perturbation at fluid 1 led to a varicose

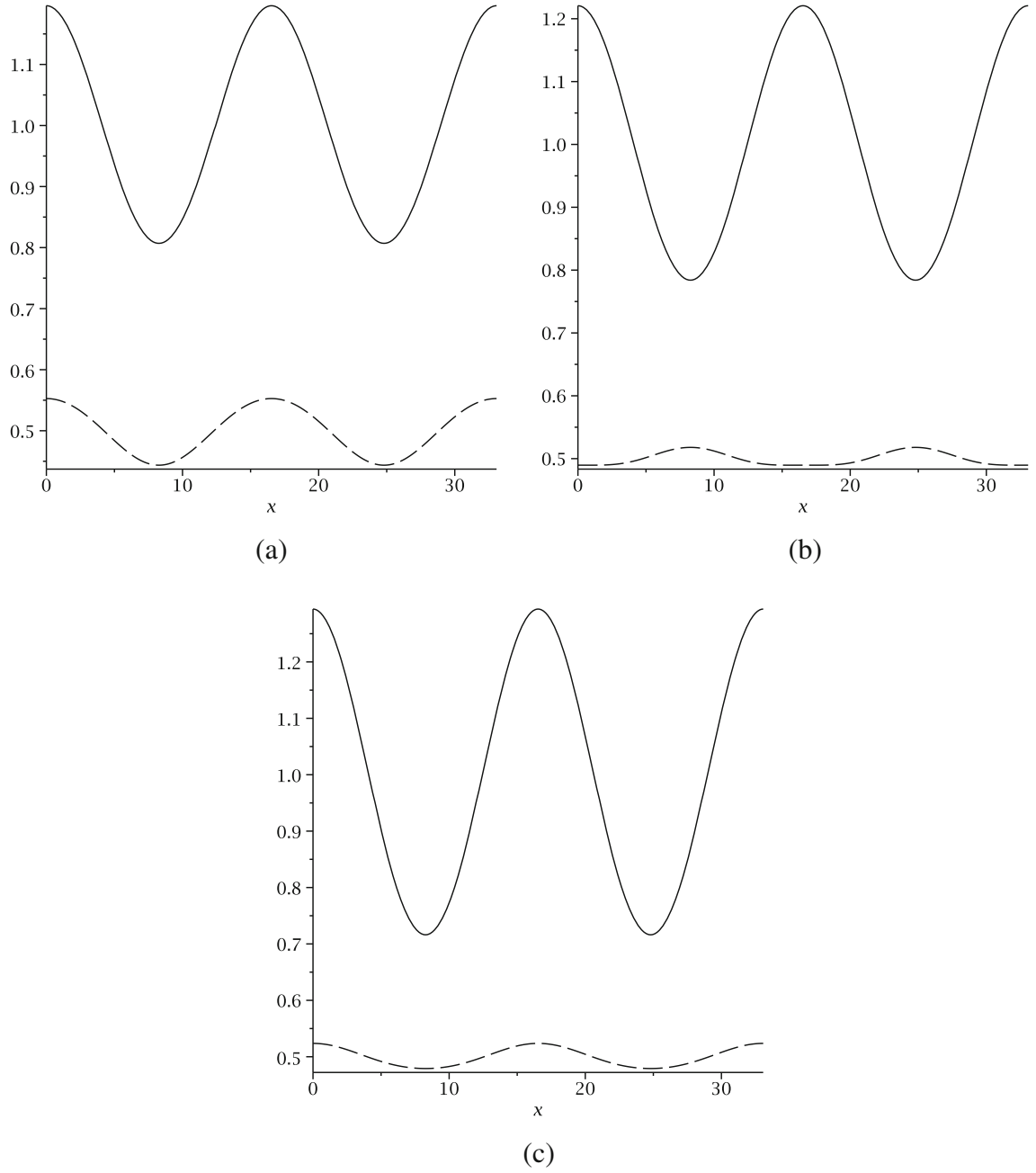

Fig. 11 Nonlinear mode: $d < 1$. Oscillatory convection. $d_w/\chi = 0.1$, $d = 0.5$, $Ma = 4.7$ ($A_p \approx 0.3$), $k = 0.38$, $\omega_p = 0.012$. **a** $A_1(0) = A_1^*(0) = 0.05$, t = 130, Sinuous. **b** $B_1(0) = B_1^*(0) = 0.05$, t = 130, Varicose. **c** $B_1(0) = B_1^*(0) = 0.05$, t = 170, Sinuous

mode (Fig. 8b, t = 300) which then (Fig. 8c) changed into a sinuous one around t = 450. After that time the mode was sinuous always.

In Fig. 9 d is increased further to $d = 0.9.A_p \approx 0.5$ and $Ma = 4.7$. The behavior of stationary convection is in agreement with previous figures. The perturbations at fluid 2 (Fig. 9a, t = 400) led to a sinuous mode of instability. However, the perturbations at fluid 1 led first (Fig. 9b, t = 400) to a varicose mode which then changed (Fig. 9c, t = 500) into a sinuous one which prevailed during the whole time.

The results of oscillatory convection when $d < 1$ are presented in the next figures. Notice in Fig. 10 that the magnitude of the perturbations $A_1(0) = A_1^*(0)$ and $B_1(0) = B_1^*(0)$ is smaller than those of the other figures. The magnitudes of the parameters used are $d = 0.1$ and $Ma = 1.5$ which gives approximately $A_p \approx 0.1$. The wavenumber is $k = 0.30$ and the corresponding frequency of oscillation is $\omega_p = 0.00075$, which is very small. It is found (Fig. 10a, t = 1500) that when perturbations are applied at fluid 2, the oscillations first start as a sinuous mode and then change into the varicose mode to again

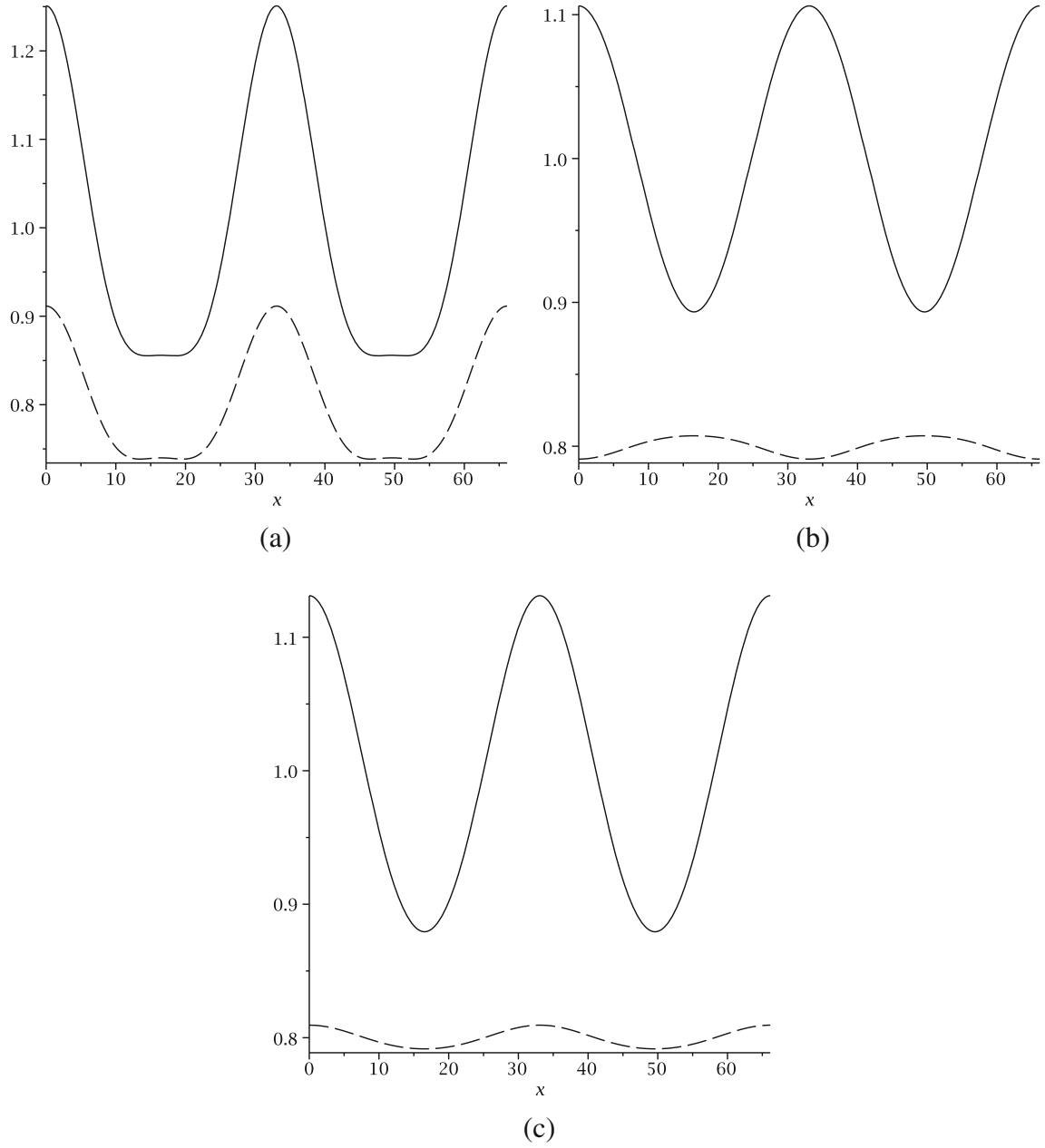

Fig. 12 Nonlinear mode: $d < 1$. Oscillatory convection. $d_w/\chi = 0.1$, $d = 0.9$, $Ma = 8.1$ ($A_p \approx 0.5$), $k = 0.19$, $\omega_p = 0.0017$. **a** $A_1(0) = A_1^*(0) = 0.05$, t = 170, Sinuous. **b** $B_1(0) = B_1^*(0) = 0.05$, t = 170, Varicose. **c** $B_1(0) = B_1^*(0) = 0.05$, t = 200, Sinuous

become a sinuous one. If the perturbations are applied at fluid 1 (Fig. 10b, t = 1500), the first mode to appear is the varicose one. Then it changes (Fig. 10c, t = 4500) into the sinuous mode and the oscillations continue from this point. It is interesting to point out that the proper and natural oscillation in fact starts around t = 4500. This means that the system first shows a varicose mode and then tries to adapt itself to the proper mode of oscillation. After that time the system starts the normal period of oscillation corresponding to the parameters selected in this Fig. 10.

Oscillatory convection was presented in Fig. 11 for different parameters. There, $d = 0.5$ and $Ma = 4.7$ were used to give $A_p \approx 0.3$. The wavenumber selected is $k = 0.38$ with a frequency of oscillation $\omega_p = 0.012$. When the perturbations were applied at fluid 2 (Fig. 11a, t = 130) the starting mode was sinuous. Then it changed into a varicose one and so forth. However, when the fluid 1 was perturbed (Fig. 11b, t = 130) the oscillations started with a varicose mode. Then the system required some time to change into a sinuous mode (Fig. 11c, t = 170). It was found that around this adaptation time the oscillations started properly with a period $2\pi/\omega_p$.

In Fig. 12 a similar behavior was found to that of the previous figures of oscillatory convection. The data were $d = 0.9$ and $Ma = 8.1$ corresponding to $A_p \approx 0.5$. In this case $k = 0.19$ and $\omega_p = 0.0017$. When perturbations are applied to fluid 2 (Fig. 12a, t = 170) the oscillations start as sinusoidal. If the perturbations are applied to fluid 1 the oscillations start as varicose (Fig. 12b, t = 170) and then change into a sinuous mode after some time (Fig. 12c, t = 200). From this time on the oscillations proceed properly with the corresponding period of oscillation.

Conclusions

The thermocapillary instability of two fluid layers thermally coupled through a solid interlayer has been investigated in the linear and nonlinear problems. The two liquid layers are supposed to be in the absence of gravity. This theoretical assumption was motivated by the possibility of an outer space experiment in a manned artificial satellite. In the linear case, it was found a quadratic equation for the growth rate. This equation had two solutions for the growth rate. The solution with largest growth rate is called the first solution. Both solutions change into an oscillatory mode after a particular wavenumber. This oscillatory wavenumber region separated two regions of the first solution which are called the first and second modes of instability. It was found that the second mode of the first solution is always stable. Therefore, it was neglected in all the discussion of the stability. The wavenumber range of oscillatory convection had a stable region which is very large for some parameters of the problem. This stable section was also neglected from the discussion.

A number of exact analytical solutions were obtained to understand in a better way the general behavior of the linear stability. Besides, some approximate solutions were obtained for the maximum growth rate of instability. These approximate solutions work correctly in a limited range of the parameters. They not necessarily work correctly for negative A_p. From the linear analytical results and their numerical confirmation, it was concluded that two sets of instability parameters were possible. The two sets are equivalent and are related to a change in sign of the Marangoni number (A_p) and to a change in magnitude of d from smaller than one to larger than one. Here, the set $A_p > 0$ and $d > 1$ and $A_p > 0$ and $d < 1$ was selected for the discussion. It was shown analytically and numerically that when $A_p > 0$ and $d > 1$, only stationary convection was possible. Moreover, only in this case stationary convection had a critical wavenumber different from zero. When $A_p > 0$ and $d < 1$, it was possible to have both stationary and oscillatory convection in different ranges of the wavenumber. It was found that stationary convection had no finite critical wavenumber. The reason was that the first mode of the first solution of the growth rate for stationary convection changed into one of oscillatory convection for a finite growth rate. Moreover, the second mode of the first solution of the growth rate was always negative an never touched the wavenumber axis. However, an analytical solution for the critical wavenumber for oscillatory convection was obtained and used to calculate a maximum frequency of unstable oscillatory convection.

A three-term expansion using the first two normal modes of the free surfaces was used in the two nonlinear evolution equations to find out which relative mode of surface deformations was preferred by the system. When $A_p > 0$ and $d > 1$ only stationary convection occurs and the nonlinear mode of instability was always sinuous, for both perturbations applied from fluid 2 and from fluid 1. When $A_p > 0$ and $d < 1$ both stationary and oscillatory convection were possible. In stationary convection it was shown that when the perturbations are applied to fluid 2 the nonlinear mode is sinuous. When they are applied to fluid 1, the first mode is varicose. Then it changes with time into a sinuous one which remains as the preferred mode. In oscillatory convection it was found that when the perturbations were applied to fluid 2 the first nonlinear mode to appear was the sinuous mode. Then the oscillations proceeded normally. When the perturbations were applied to fluid 1 the oscillations started with a varicose mode. Then, they changed with time into a sinuous mode. It is interesting that the proper oscillations of the system started to occur just after the oscillations became sinuous. That is, it seems that the period of oscillation started at that time. The conclusion

is that when perturbations are applied form fluid 1, the system with a varicose mode needs a time to adapt itself to the conditions imposed by the parameters and then it starts the proper oscillations as sinuous. From that moment, in a period $2\pi/\omega_p$ the system will have again a varicose mode, and so forth.

A rich variety of phenomena occur when the fluid layers have a thermal coupling by means of a wall with finite thickness and thermal conductivity. Here, some of the parameters have been fixed to make the system more easier to understand. However, a number of interesting phenomena have been found as a result of the two layers interaction, even when the two fluids are the same and the atmospheres are the same but with different temperatures. As a next step, it is of interest to include the effect of gravity. This problem is already in preparation.

Acknowledgments The author would like to thank Prof. Stephen Muhl Saunders for reviewing the whole text of the paper. Also thanks are due to Alberto López, Alejandro Pompa, Cain González, Raúl Reyes, Ma. Teresa Vázquez and Oralia Jiménez for technical support.

References

Catton, I., Lienhard, J.H., V: Thermal stability two fluid layers separated by a solid interlayer of finite thickness and thermal conduclivity. J. Heat Transf. **106**, 605–612 (1984)

Char, M.-I., Chen, C.-C.: Influence of viscosity variation on the stationary Bénard-Marangoni instability with a boundary slab of finite conductivity. Acta Mech. **135**, 181–198 (1999)

Dávalos-Orozco, L.A.: Thermocapillar instability of liquid sheets in motion. Colloids Surf. A **157**, 223–233 (1999)

Dávalos-Orozco, L.A.: Thermal Marangoni convection of a fluid film coating a deformable membrane. J. Colloid Interface Sci. **234**, 106–116 (2001)

Dávalos-Orozco, L.A.: The effect of the thermal conductivity and thickness of the wall on the nonlinear instability of a thin film flowing down an incline. Int. J. Nonlinear Mech. **47**, 1–7 (2012)

Dávalos-Orozco, L.A.: Nonlinear instability of a thin film flowing down a smoothly deformed thick wall of finite thermal conductivity. Interfacial Phenom. Heat Transf. **2**, 55–74 (2014)

Dávalos-Orozco, L.A.: Non-linear instability of a thin film flowing down a cooled wavy thick wall of finite thermal conductivity. Phys. Lett. A **379**, 962–967 (2015)

Dávalos-Orozco, L.A.: Thermal Marangoni instability of a thin film flowing down a thick wall deformed in the backside. Phys. Fluids **28**(054103), 1–12 (2016)

Dávalos-Orozco, L.A., You, X.-Y.: Three-dimensional instability of a liquid layer flowing down a heated vertical cylinder. Phys. Fluids **12**, 2198–2209 (2000)

Fu, Q.-F., Yang, L.-J., Tong, M.-X., Wang, C.: Absolute and convective instability of a liquid sheet with transverse temperature gradient. Int. J. Heat Fluid Flow **44**, 652–661 (2013)

Gangadharaiah, Y.H.: Onset of surface tension driven convection in a fluid layer with a boundary slab of finite conductivity and deformable free surface. Int. J. Math Archive **4**, 311–323 (2013)

Getachew, D., Rosenblat, S.: Thermocapillary instability of a viscoelastic liquid layer. Acta Mech. **55**, 137–149 (1985)

Hernández Hernández, I.J., Dávalos-Orozco, L.A.: Competition between stationary and oscillatory viscoelastic thermocapillary convection of a film coating a thick wall. Int. J. Thermal Sci. **89**, 164–173 (2015)

Kabova, Y.O., Alexeev, A., Gambaryan-Roisman, T., Stephan, P.: Marangoni-induced deformation and rupture of a liquid film on a heated microstructured wall. Phys. Fluids **18**, 012104 (2006)

Kalitzova-Kurteva, P.G., Slavtchev, S.G., Kurtev, I.A.: Stationary Marangoni instability in a liquid layer with temperature-dependent viscosity and deformable free surface. Microgravity Sci. Technol. **9**, 257–263 (1996)

Lienhard, J.H., V, Catton, I.: Heat transfer across a two-fluid-layer region. J. Heat Transf. **108**, 198–205 (1986)

Mctaggart, C.L.: Convection driven by concentration and temperature dependent surface tension. J. Fluid Mech. **134**, 301–310 (1983)

Moctezuma-Sánchez, M., Dávalos-Orozco, L.A.: Azimuthal instability modes in a viscoelastic liquid layer flowing down a heated cylinder. Int. J. Heat Mass Transf. **90**, 15–25 (2015)

Oron, A., Deissler, R.J., Duh, J.C.: Marangoni instability in a liquid layer with two free surfaces. Eur. J. Mech. B/Fluids **14**, 737–760 (1995a)

Oron, A., Deissler, R.J., Duh, J.C.: Marangoni instability in a liquid sheet. Adv. Space Res. **16**, 83–86 (1995b)

Oron, A., Davis, S.H., Bankoff, S.G.: Long scale evolution of thin liquid films. Rev. Mod. Phys. **69**, 931–980 (1997)

Pearson, J.R.A.: On convection cells induced by surface tension. J. Fluid Mech. **4**, 482–500 (1958)

Scriven, L.E., Sternling, C.V.: On cellular convection driven by surface-tension gradients: effects of means surface tension and surface viscosity. J. Fluid Mech. **19**, 321–340 (1964)

Simanovskii, I., Viviani, A., Dubois, F., Legros, J.-C.: Nonlinear buoyant-thermocapillary waves in two-layer systems with an interfacial heat release. Microgravity Sci. Technol. **27**, 11–26 (2015)

Simanovskii, I., Nepomnyashchy, A., Viviani, A., Dubois, F.: Nonlinear waves in two-layer systems with a temperature-dependent interfacial heat release. Microgravity Sci. Technol. **28**, 381–393 (2016)

Slavtchev, S., Ouzounov, V.: Stationary Marangoni instability in a liquid layer with temperature-dependent viscosity in microgravity. Microgravity Q. **4**, 33–38 (1994)

Slavtchev, S.G., Kalitzova-Kurteva, P.G., Kurtev, I.A.: Oscillatory Marangoni instability in a liquid layer with temperature-dependent viscosity and deformable free surface. Microgravity Sci. Technol. **11**, 29–34 (1998)

Takashima, M.: Surface-tension driven convection with boundary slab of finite conductivity. J. Phys. Soc. Jpn. **29**, 531–531 (1970)

Takashima, M.: Surface tension driven instability in a horizontal liquid layer with a deformable free surface. I. Stationary convection. J. Phys. Soc. Jpn. **50**, 2745–2750 (1981a)

Takashima, M.: Surface tension driven instability in a horizontal liquid layer with a deformable free surface. II. Overstability. J. Phys. Soc. Jpn **50**, 2751–2756 (1981b)

Tong, M.-X., Yang, L.-J., Fu, Q.-F.: Thermocapillar instability of a two-dimensional viscoelastic planar liquid sheet in surrounding gas. Phys. Fluids **26**(033105), 1–14 (2014)

Yang, H.Q.: Boundary effect on the Bénard-Marangoni instability. Int. J. Heat Mass Transf. **35**, 2413–2420 (1992)